High precision mass measurements for tests of QED and search for dark matter at PENTATRAP

Menno Door

Max Planck Institute for Nuclear Physics, Heidelberg

2023/06/09

Max Planck Society

IMPRS-PTFS

DFG FOR 2202

ERC AdG 832848 - FunI

DFG SFB 1225

MAX-PLANCK-INSTITUT FÜR KERNPHYSIK

Outline

- Penning Trap introduction
- Pentatrap Setup
- Absolute mass measurements (Test of QED)
- Isotope chain mass-ratios (search for 5th force)

Pentatrap Lab/Magnet and Trap Tower

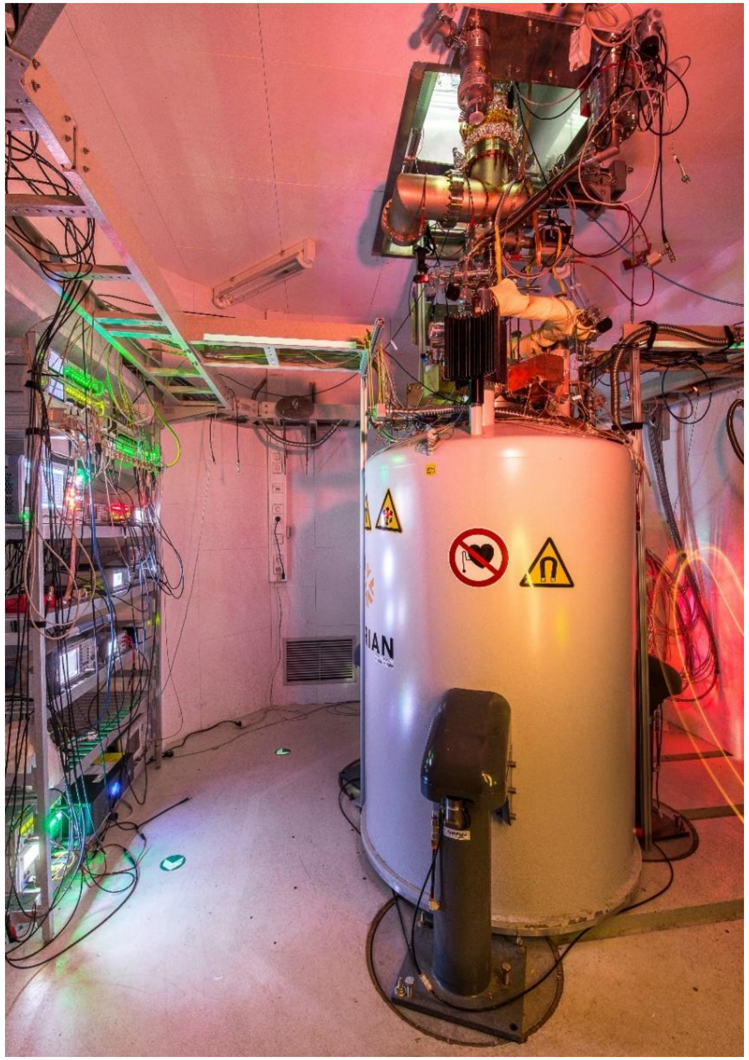

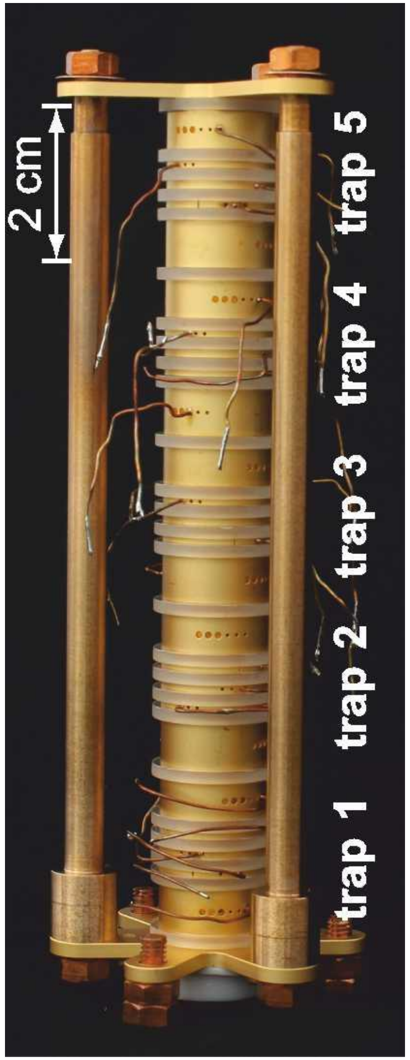

Penning-trap

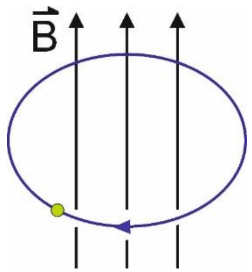

+

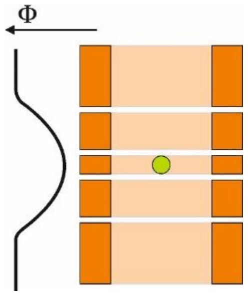

=

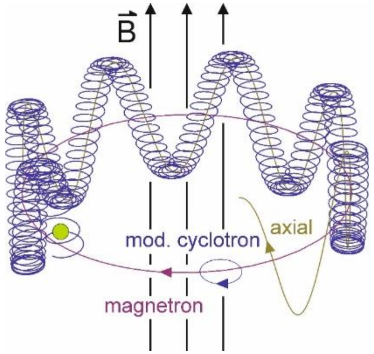

Free-space
cyclotron frequency

Harmonic electrical
potential

3 Eigenmotions in trap

$$\boxed{\omega_c = \frac{qB}{m}}$$

$$\omega_z = \sqrt{\frac{2qC_2}{md^2}U}$$

$$\omega_+ = \frac{\omega_c}{2} + \sqrt{\frac{\omega_c^2}{4} - \frac{\omega_z^2}{2}}$$

$$\omega_- = \frac{\omega_c}{2} - \sqrt{\frac{\omega_c^2}{4} - \frac{\omega_z^2}{2}}$$

Measurement of all Eigenfrequencies

$$\boxed{\omega_c^2 = \omega_+^2 + \omega_z^2 + \omega_-^2}$$

Rev. Mod. Phys. 58, 233 (1986)

Penning-trap

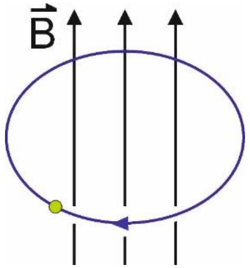

+

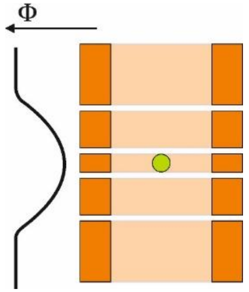

=

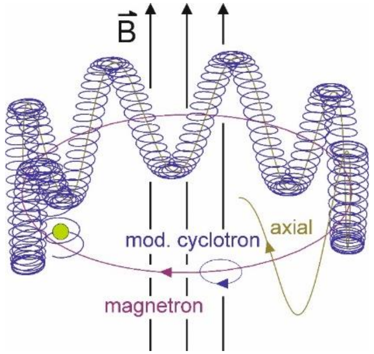

Free-space
cyclotron frequency

$$\boxed{\omega_c = \frac{qB}{m}}$$

Harmonic electrical
potential

3 Eigenmotions in trap

$$\omega_z = \sqrt{\frac{2qC_2}{md^2}U}$$

$$\omega_+ = \frac{\omega_c}{2} + \sqrt{\frac{\omega_c^2}{4} - \frac{\omega_z^2}{2}}$$

$$\omega_- = \frac{\omega_c}{2} - \sqrt{\frac{\omega_c^2}{4} - \frac{\omega_z^2}{2}}$$

Measurement of all Eigenfrequencies

$$\boxed{\omega_c^2 = \omega_+^2 + \omega_z^2 + \omega_-^2}$$

Rev. Mod. Phys. 58, 233 (1986)

Mass Spectrometry

$$\boxed{\omega_c^2 = \omega_+^2 + \omega_z^2 + \omega_-^2}$$ Ion A

Ion B $$\boxed{\omega_c^2 = \omega_+^2 + \omega_z^2 + \omega_-^2}$$

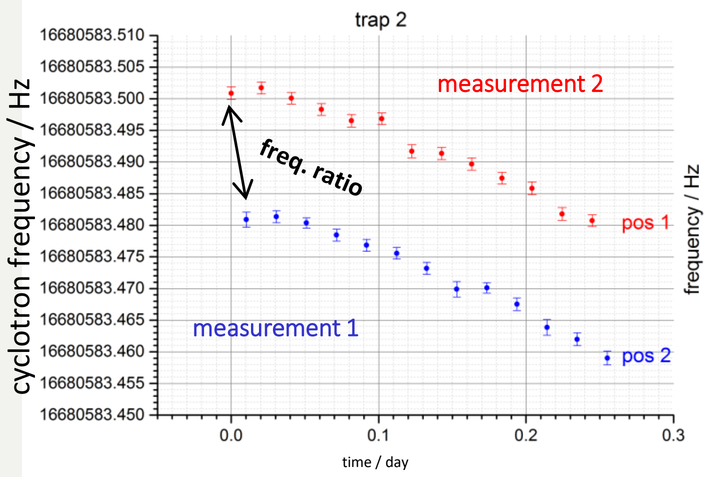

Mass ratio: $$\boxed{R = \frac{\omega_c^A}{\omega_c^B} = \frac{q^A m^B}{q^B m^A}}$$

Fourier transform ion cyclotron resonance – FT-ICR

measurement of ν_z with dip

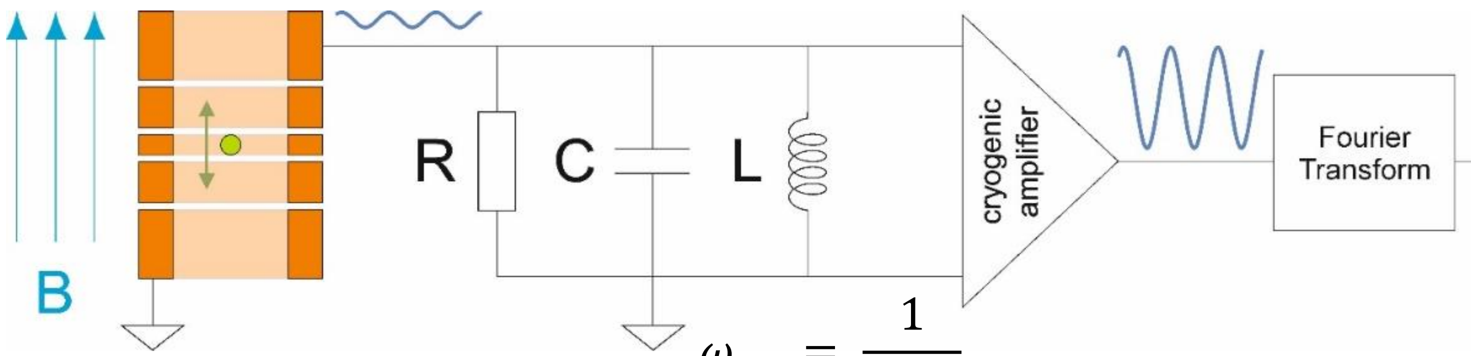

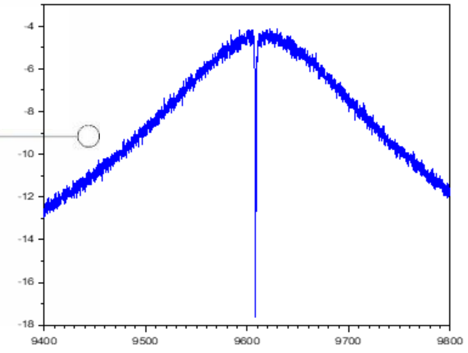

$$\omega_{res} = \frac{1}{\sqrt{LC}}$$

Direct measurement of ω_z by dip method

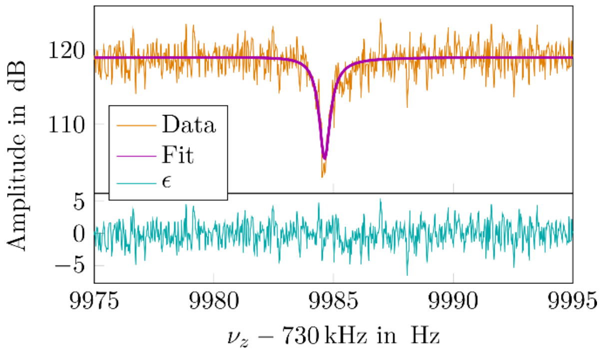

$$\omega_z = \sqrt{\frac{2qC_2}{md^2}U} \cong \omega_{res}$$

Fourier transform ion cyclotron resonance – FT-ICR

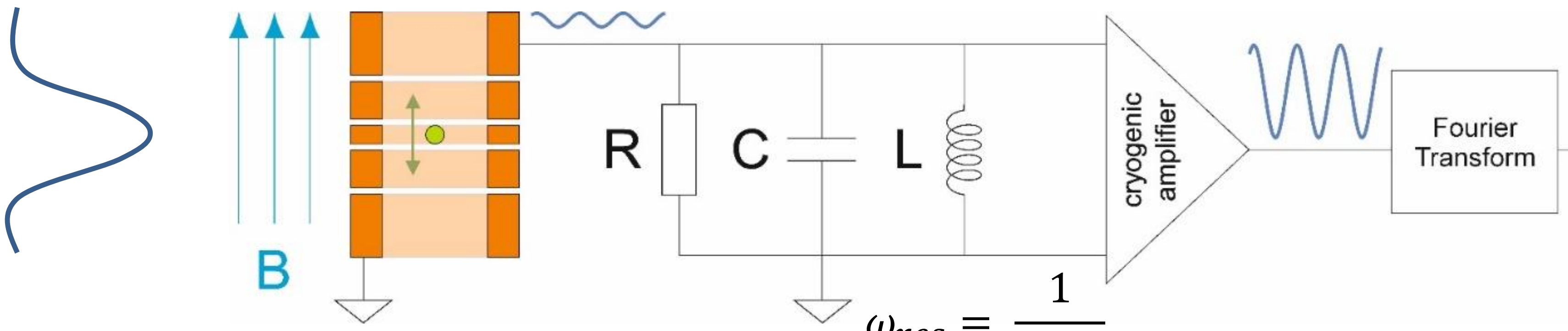

$$\omega_{res} = \frac{1}{\sqrt{LC}}$$

measurement of ν_z with dip

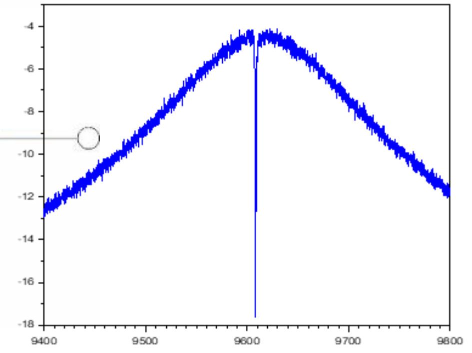

Direct measurement of ω_z by dip method

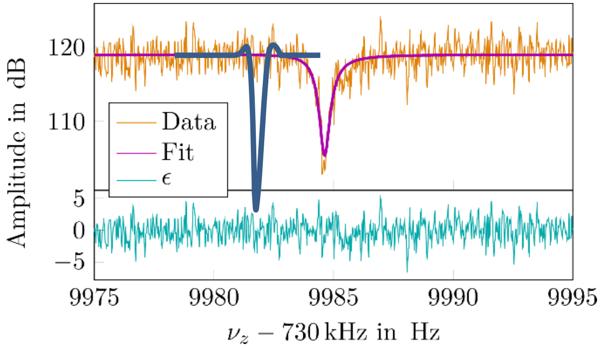

$$\omega_z = \sqrt{\frac{2qC_2}{md^2}U} \cong \omega_{res}$$

Fourier transform ion cyclotron resonance – FT-ICR

measurement of ν_z with dip

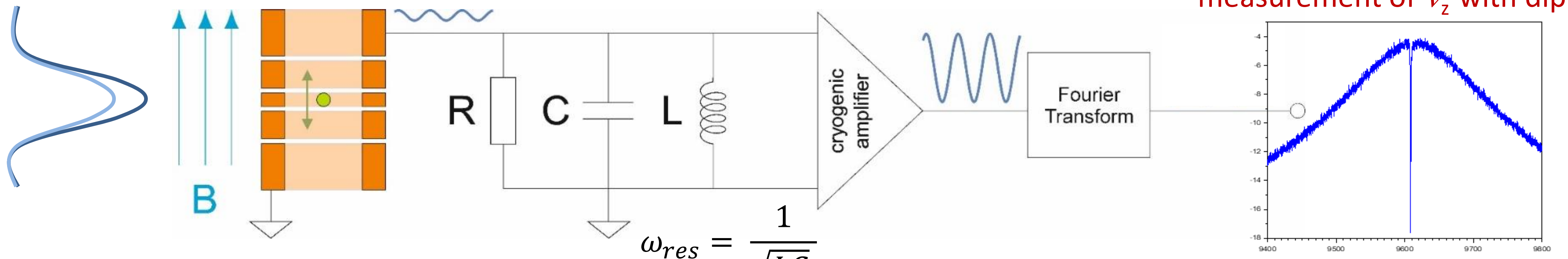

$$\omega_{res} = \frac{1}{\sqrt{LC}}$$

Direct measurement of ω_z by dip method

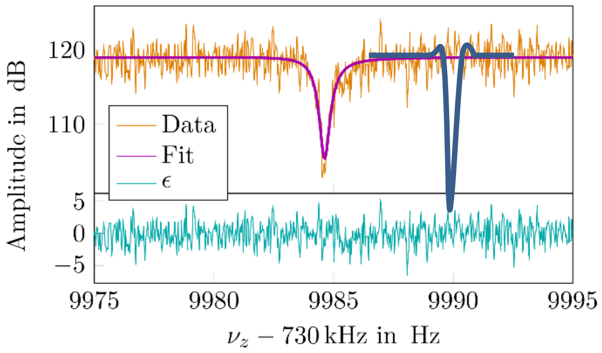

$$\omega_z = \sqrt{\frac{2qC_2}{md^2}U} \cong \omega_{res}$$

Fourier transform ion cyclotron resonance – FT-ICR

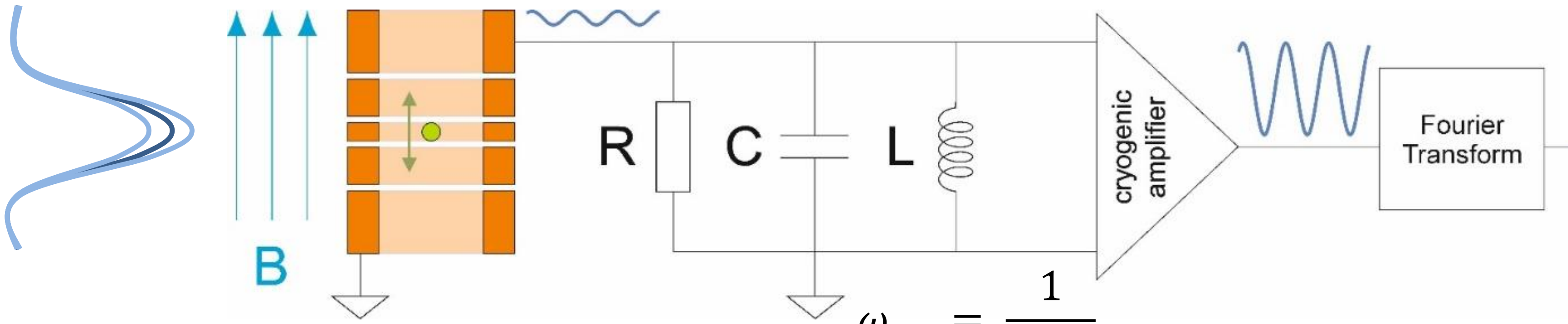

$$\omega_{res} = \frac{1}{\sqrt{LC}}$$

measurement of ν_z with dip

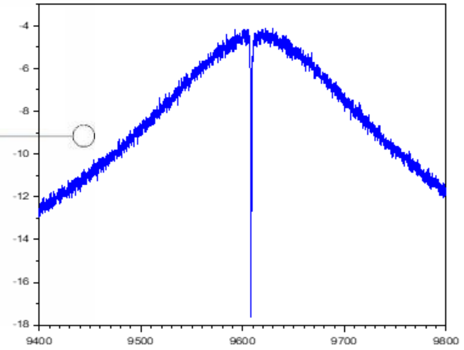

Direct measurement
of ω_z by dip method

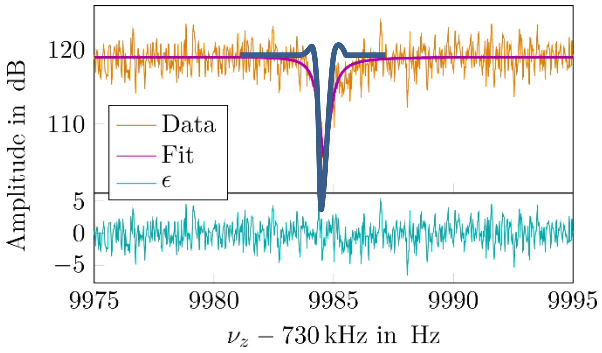

$$\omega_z = \sqrt{\frac{2qC_2}{md^2}U} = \omega_{res}$$

Fourier transform ion cyclotron resonance – FT-ICR

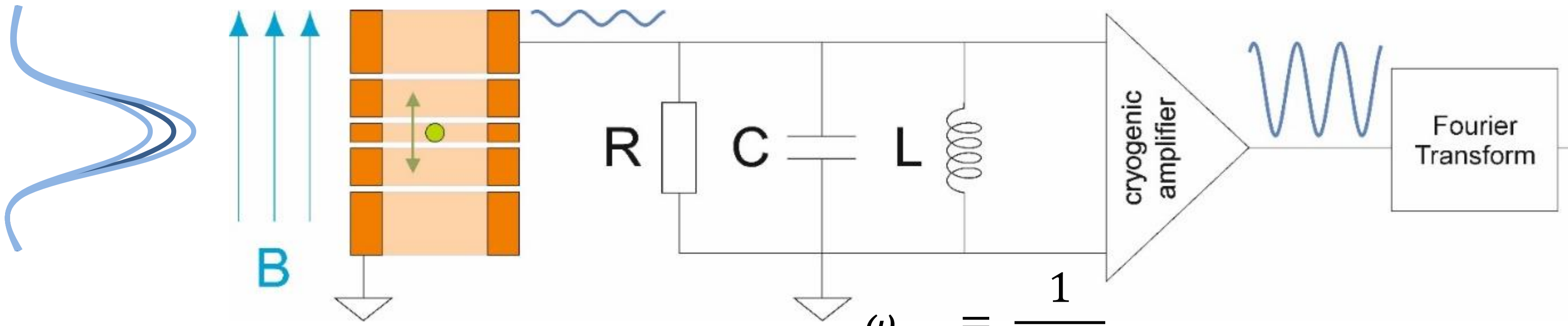

$$\omega_{res} = \frac{1}{\sqrt{LC}}$$

measurement of ν_z with dip

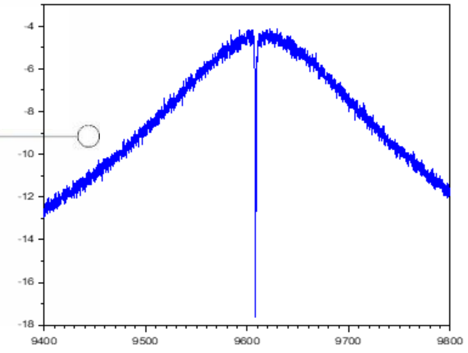

Direct measurement of ω_z by dip method

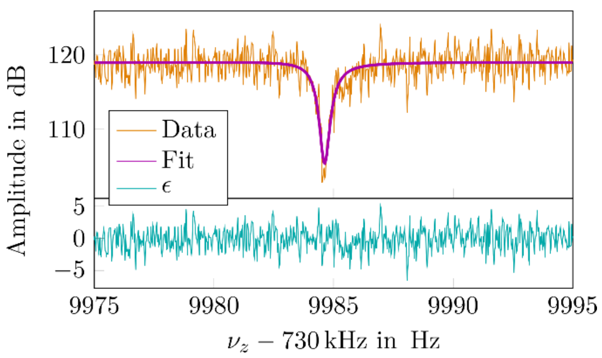

$$\omega_z = \sqrt{\frac{2qC_2}{md^2}U} = \omega_{res}$$

Indirect measurement of $\omega_{+/-}$ by double dip method

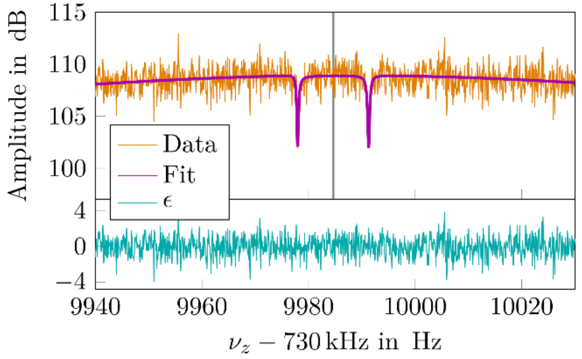

Sideband coupling ω_- to ω_z (coupled harmonic oscillators)

Fourier transform ion cyclotron resonance – FT-ICR

measurement of ν_z with dip

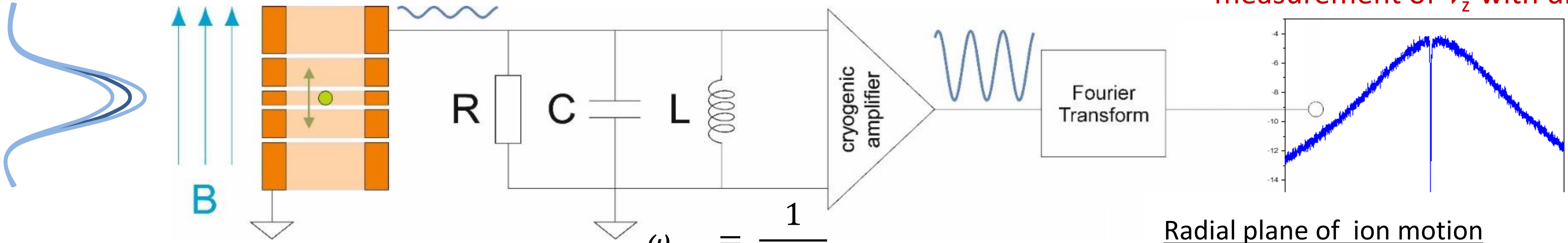

$$\omega_{res} = \frac{1}{\sqrt{LC}}$$

Direct measurement of ω_z by dip method

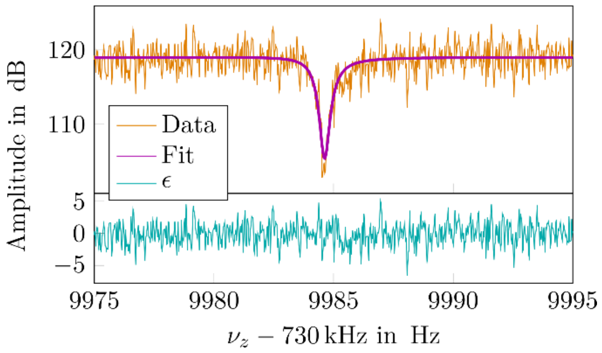

$$\omega_z = \sqrt{\frac{2qC_2}{md^2}U} = \omega_{res}$$

Indirect measurement of $\omega_{+/-}$ by double dip method

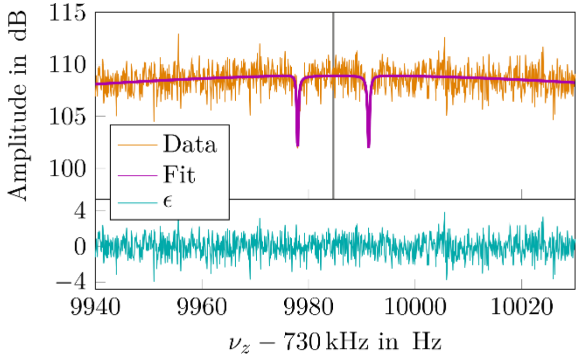

Sideband coupling ω_- to ω_z (coupled harmonic oscillators)

ω_+: phase sensitive method „**Pulse and Phase / PnP**"

Far more precise then double dip method

Ramsey type measurement

Radial plane of ion motion

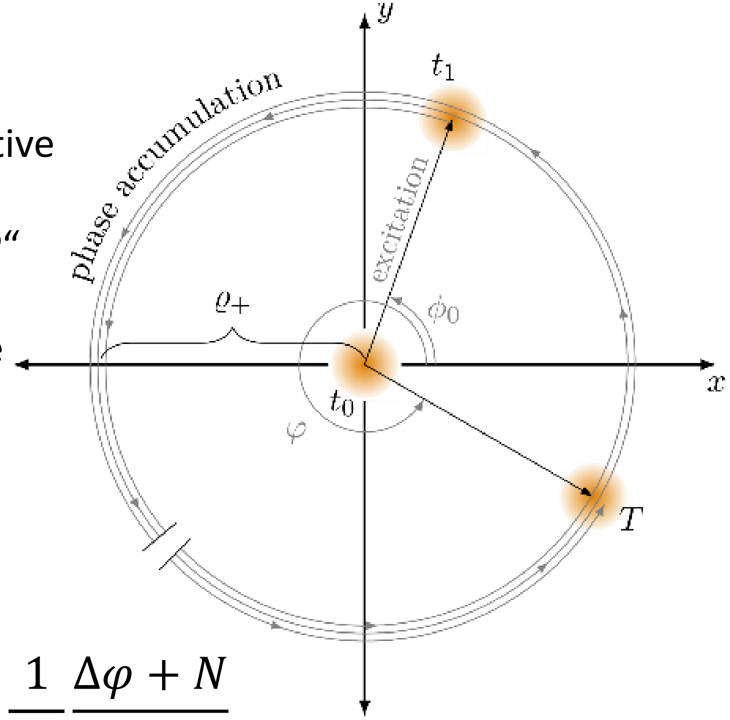

$$\omega_+ = \frac{1}{2\pi}\frac{\Delta\varphi + N}{\Delta T}$$

Outline

- ~~Penning Trap introduction~~
- Pentatrap Setup
- Absolute mass measurements (Test of QED)
- Isotope chain mass-ratios (search for 5th force)

Pentatrap Lab/Magnet and Trap Tower

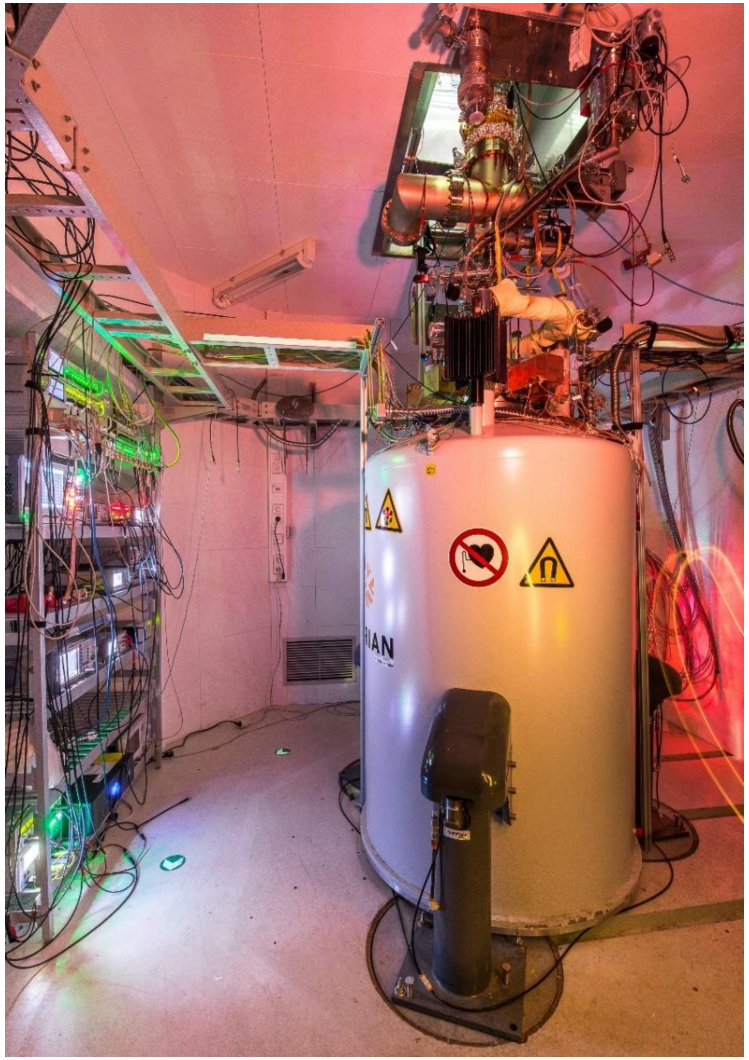

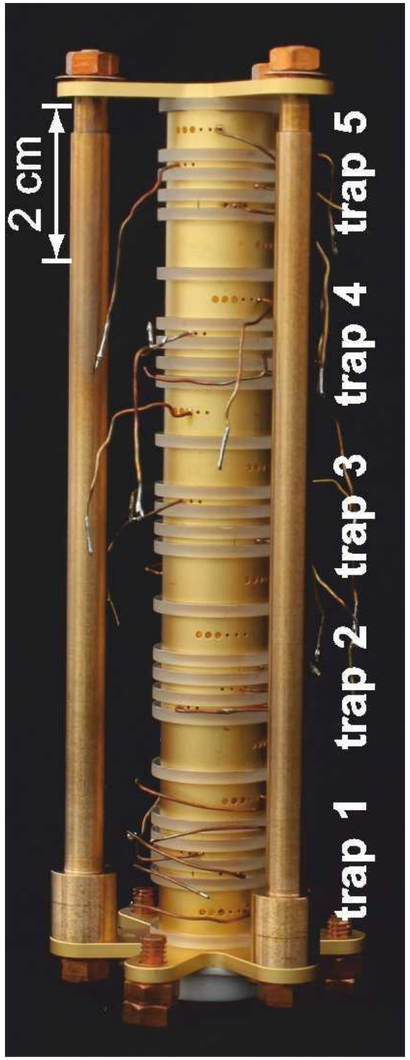

Pentatraps unique features

- **Stack of five identical Penning traps**
- Cryogenic environment (4.2 K)
- 7 T superconducting magnet with vertical cold bore
- Temperature in the lab is stabilized: ± 0.05 K/day
- LHe-level in the bore is stabilized: ± 50 μm
- He-pressure in the bore is stabilized: ± 2 μbar
- Relative stability of *B*-field: 10^{-10} / hour
- Ultra-stable voltage source: $\Delta U/U < 10^{-7}$ / 100 s
- **Highly charged ions (!!!): $\omega_c \geq 20\ MHz$**
- **Simultaneous measurement of ω_+ and ω_z**
- **Tunable detection system, $\omega_{res} \pm 6\ kHz$**

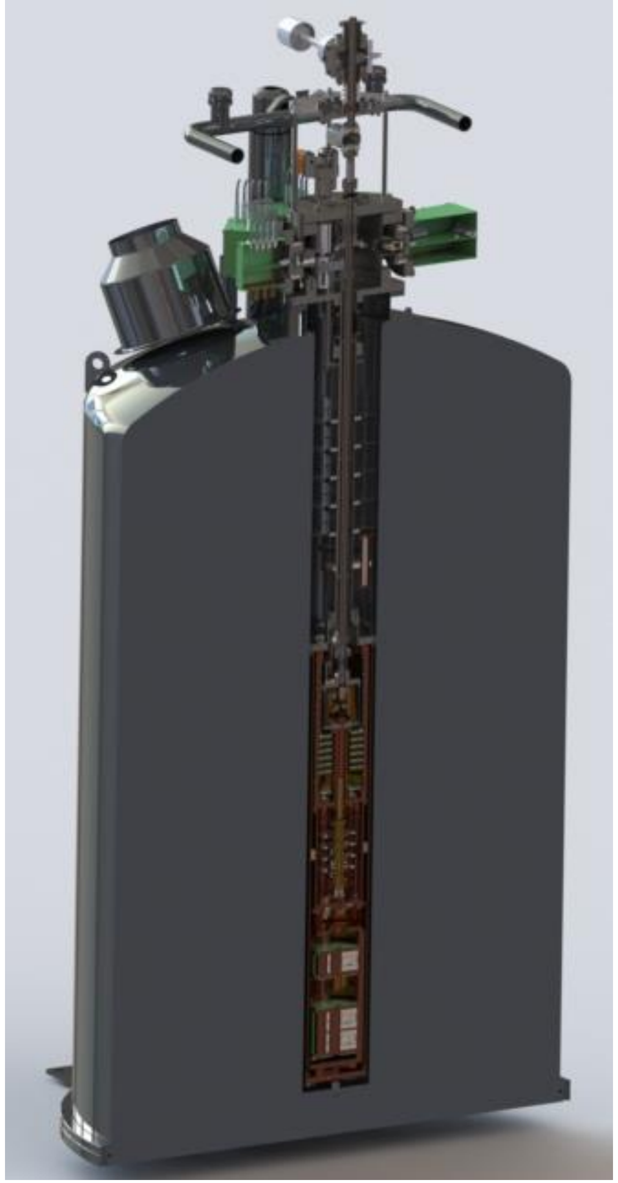

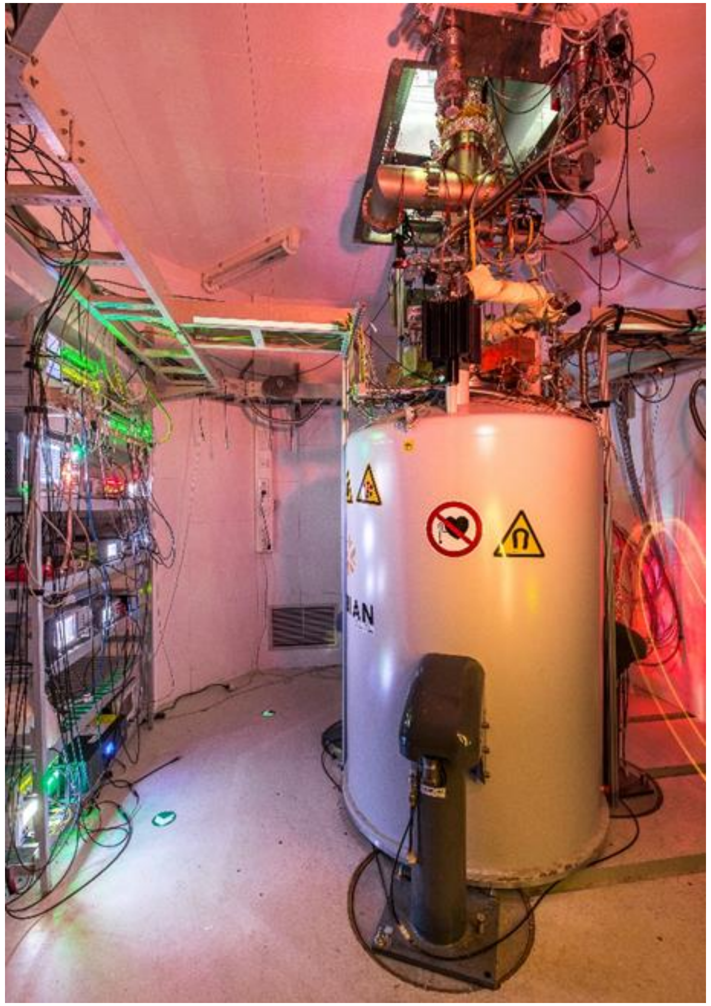

Repp, J. et al., Appl. Phys. B 107, 983 (2012)
Roux, C. et al., Appl. Phys. B 107, 997 (2012)
Böhm, C. et al., Nucl. Instrum. Meth. A 828, 125 (2016)

Simultaneous measurement in two traps – nice to check systematics

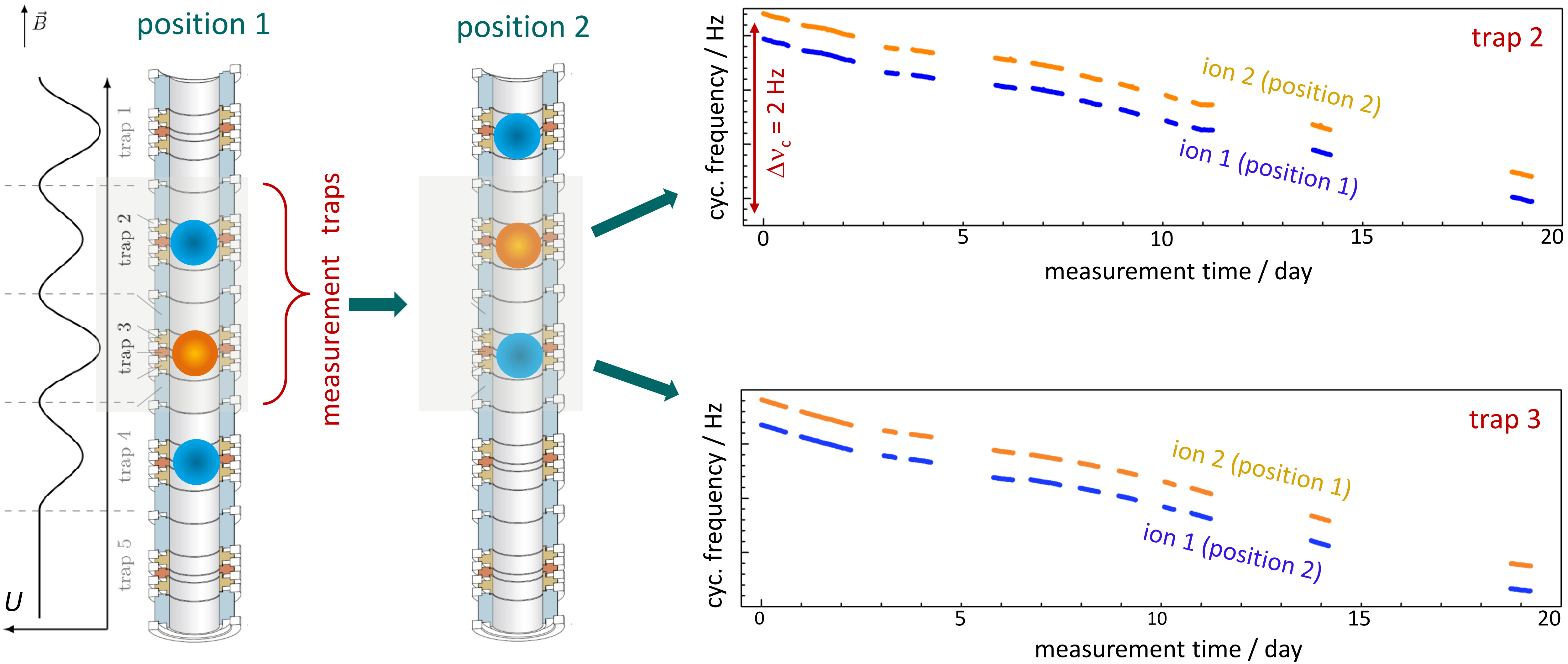

Pulse and Phase measurement with simulatenous axial dip

simultaneous measurement of ν_+ (**PnP**) and ν_z(**dip**)

excitation of ν_+ motion
(from 1 μm to 10 μm)

measurement of
accumulated $\Delta\phi_+$

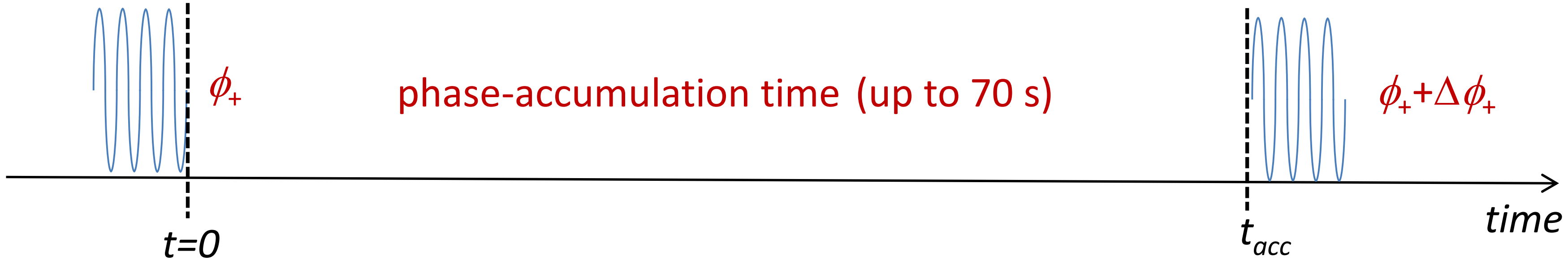

$$\nu_+ = \frac{\Delta\phi_+ + 2\pi N}{2\pi t_{acc}}$$

measurement of ν_z with dip

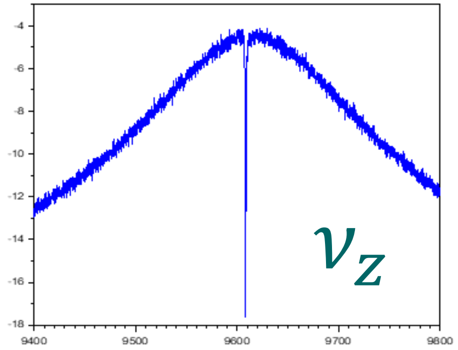

E. A. Cornell *et al.*, Phys. Rev. Letter 63 (1989) 1674

D. J. Wineland and H. G. Dehmelt, J. of Appl. Phys. 46 (1975) 919

Tunable detection system: ω_{res} is adjusted instead of ω_z/U_{trap}

Both ions at same potential depth during measurement

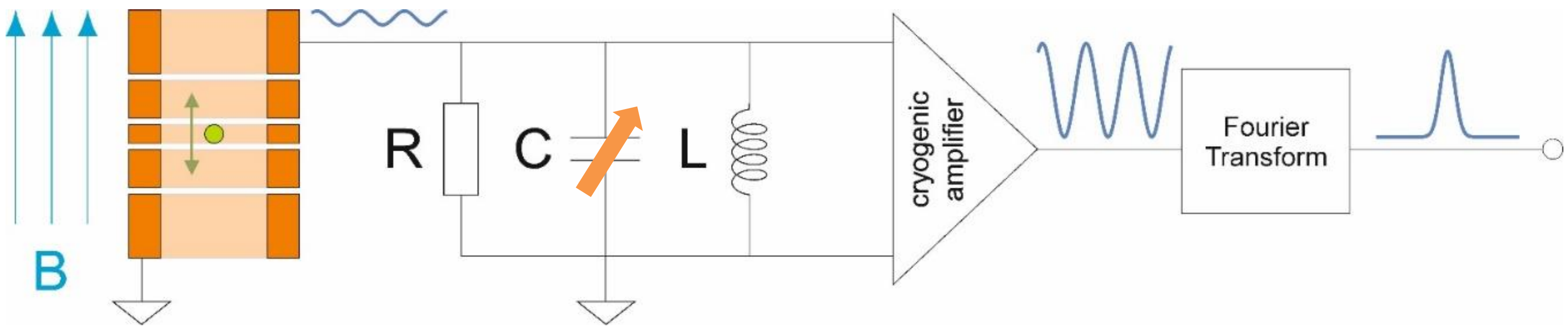

Helps if you have systematic effects due to trap asymmetries and B1 magnetic field gradient

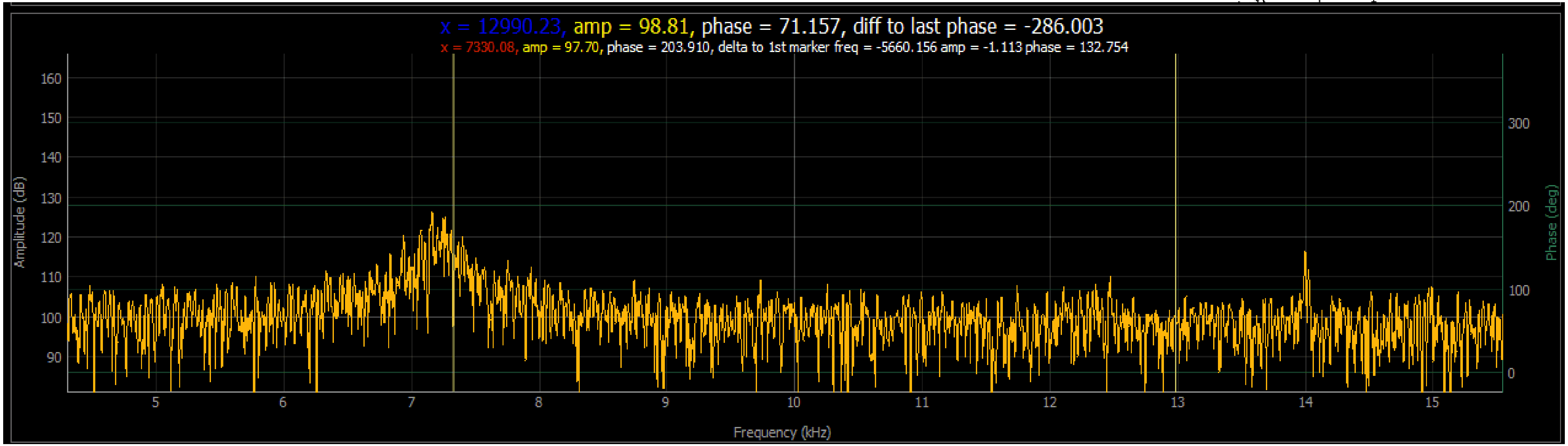

Outline

- ~~Penning Trap introduction~~
- ~~Pentatrap Setup~~
- Absolute mass measurements (Test of QED)
- Isotope chain mass-ratios (search for 5th force)

Pentatrap Lab/Magnet and Trap Tower

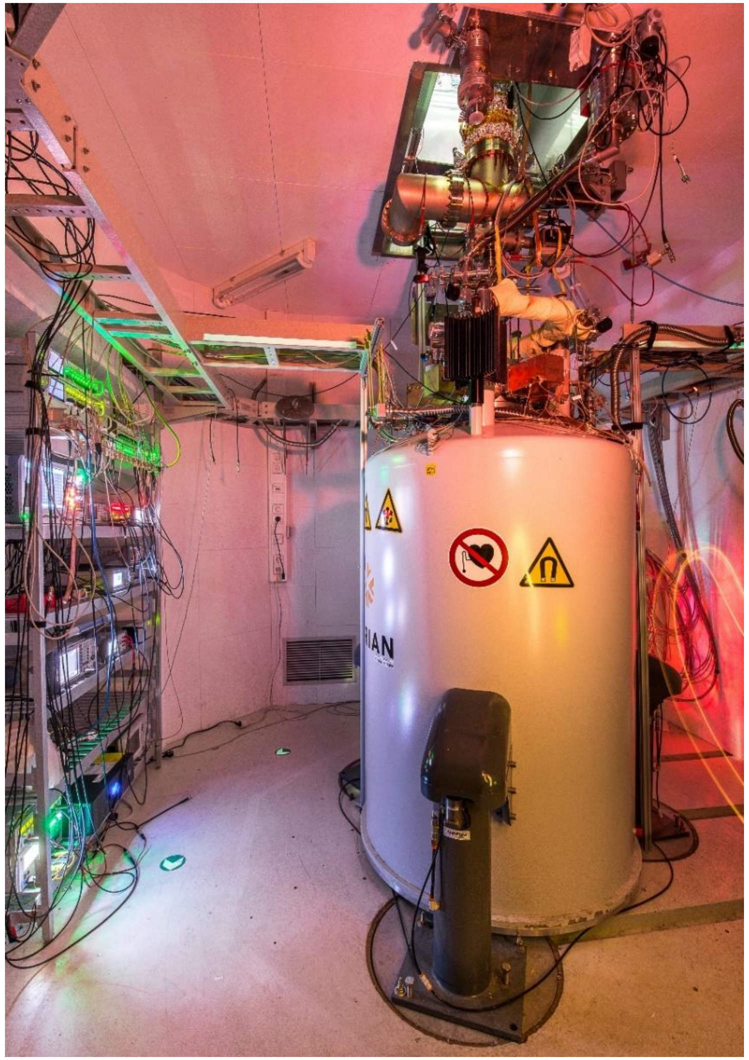

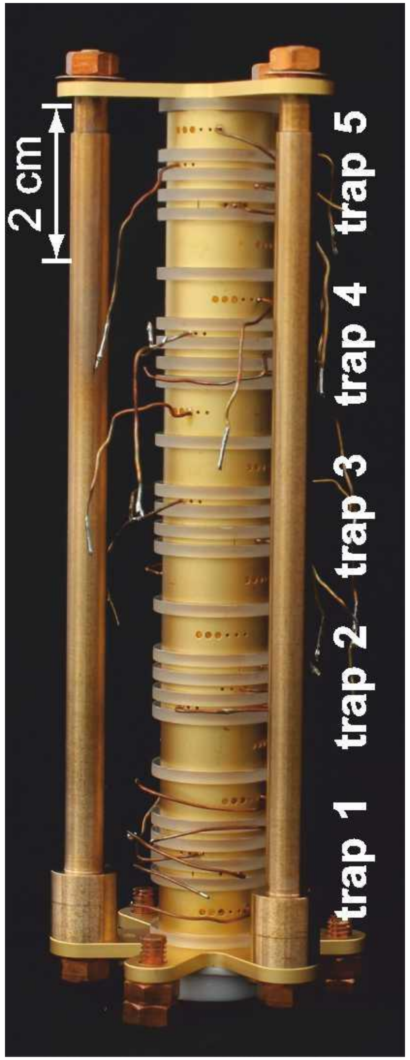

Pentatrap Motivation: Applications of mass-ratios $\delta m/m \leq 10^{-11}$

Neutrino physics

$$^{187}\mathrm{Re} \rightarrow {}^{187}\mathrm{Os} + e^- + \overline{\nu_e} + Q_{\beta^-}$$

$$^{163}\mathrm{Ho} + e^- \rightarrow {}^{163}\mathrm{Dy} + \nu_e + Q_{EC}$$

Gastaldo, L. et al., Eur. Phys. J. ST 226, 1623 (2017)

Filianin, P. et al., Phys. Rev. Lett. 127, 072502 (2021) $\delta Q = 1.3\ \mathrm{eV}$

In preparation, Schweiger, Ch. Nature (2023) $\delta Q = 0.8\ \mathrm{eV}$

Meta-stable states for HCI clocks

$$\Delta m({}^{208}\mathrm{Pb}^{41+} - {}^{208}\mathrm{Pb}^{*41+})$$

$$\Delta m({}^{187}\mathrm{Re}^{29+} - {}^{187}\mathrm{Re}^{*29+})$$

Kozlov, M. G. et al., Rev. Mod. Phys. 90, 045005 (2018)

Submitted, Kromer, K. (2023)

Schuessler, R. X. et al., Nature 581, 42 (2020)

Test of QED

Binding energies: $E_B(\mathrm{Xe}^{17+}) = \Delta m(\mathrm{Xe}^{17+} - \mathrm{Xe}^{18+})c^2 - m_e c^2$

g-factor: $g = 2\dfrac{\nu_L}{\nu_c}\dfrac{m_e}{m({}^{20}\mathrm{Ne})}\dfrac{q}{e}$

Shabaev, V. M. et al., Int. J. of Mass Spec. 251, 109, (2006)

Rischka, A. et al., Phys. Rev. Lett. 124, 113001 (2020)

Submitted, Heisse, F. (2023)

Dark Matter search: Isotope shift

$$\nu_i^{AA'} = K_i\,\boldsymbol{\mu}_{AA'} + F_i\,\delta\langle r^2\rangle_{AA'} + \alpha_{NP}X_i\gamma_{AA'}$$

Flambaum, V. V. et al., Phys. Rev. A 79, 032510 (2018)

Yb isotope mass-ratios done, Ca isotopes currently being measured

Test of $E = mc^2$

$$E = \frac{hc}{\lambda} = \Delta m({}^{36}\mathrm{Cl} - {}^{35}\mathrm{Cl} - n)c^2$$

Rainville, S. et al., Nature 438, 1096 (2005)

Pentatrap Motivation: Applications of mass-ratios $\delta m/m \leq 10^{-11}$

Neutrino physics

$$^{187}\mathrm{Re} \rightarrow {}^{187}\mathrm{Os} + e^- + \overline{\nu_e} + Q_{\beta^-}$$

$$^{163}\mathrm{Ho} + e^- \rightarrow {}^{163}\mathrm{Dy} + \nu_e + Q_{EC}$$

Gastaldo, L. et al., Eur. Phys. J. ST 226, 1623 (2017)

→ Filianin, P. et al., Phys. Rev. Lett. 127, 072502 (2021) — $\delta Q = 1.3$ eV

→ In preparation, Schweiger, Ch. Nature (2023) — $\delta Q = 0.8$ eV

Meta-stable states for HCI clocks

$$\Delta m({}^{208}\mathrm{Pb}^{41+} - {}^{208}\mathrm{Pb}^{*41+})$$

$$\Delta m({}^{187}\mathrm{Re}^{29+} - {}^{187}\mathrm{Re}^{*29+})$$

Kozlov, M. G. et al., Rev. Mod. Phys. 90, 045005 (2018)

→ *Submitted, Kromer, K. (2023)*

→ Schuessler, R. X. et al., Nature 581, 42 (2020)

Test of QED

Binding energies: $E_B(\mathrm{Xe}^{17+}) = \Delta m(\mathrm{Xe}^{17+} - \mathrm{Xe}^{18+})c^2 - m_e c^2$

→ Rischka, A. et al., Phys. Rev. Lett. 124, 113001 (2020)

g-factor: $g = 2\dfrac{\nu_L}{\nu_c}\dfrac{m_e}{m({}^{20}\mathrm{Ne})}\dfrac{q}{e}$

Shabaev, V. M. et al., Int. J. of Mass Spec. 251, 109, (2006)

→ *Submitted, Heisse, F. (2023)*

Dark Matter search: Isotope shift

$$\nu_i^{AA'} = K_i\,\boldsymbol{\mu}_{AA'} + F_i\,\delta\langle r^2\rangle_{AA'} + \alpha_{NP}X_i\gamma_{AA'}$$

Flambaum, V. V. et al., Phys. Rev. A 79, 032510 (2018)

→ **Yb isotope mass-ratios done, Ca isotopes currently being measured**

Test of $E = mc^2$

$$E = \frac{hc}{\lambda} = \Delta m({}^{36}\mathrm{Cl} - {}^{35}\mathrm{Cl} - n)c^2$$

Rainville, S. et al., Nature 438, 1096 (2005)

20Ne mass measurement – Test of QED in strong fields

light non-mass doublet

$$R \equiv \frac{\nu_c(Ne)}{\nu_c(C)} = Function\left(\frac{\rho_+(Ne)-\rho_+(C)}{\rho_+}\right)$$

R was measured at several ρ_+ values

extrapolation to $\rho_+ = 0$

$$\delta R_{\rho_+=0} \approx 10^{-11}$$

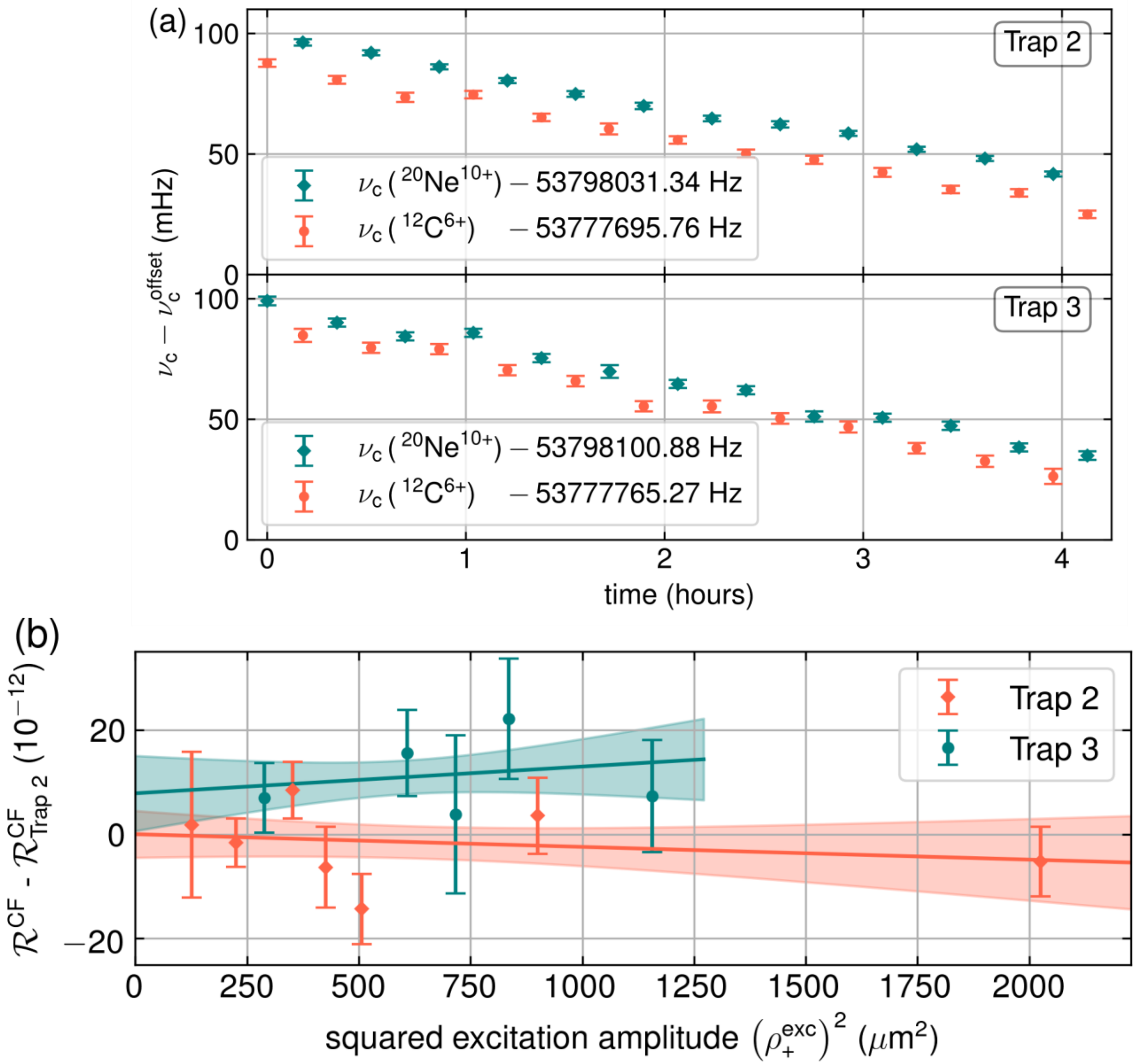

20Ne mass measurement – Test of QED in strong fields

$$g_{\text{exp}} = 2\,\frac{\nu_L}{\nu_c}\,\frac{m_e}{m\left({}^{20}_{10}Ne\right)}\,\frac{q}{e}$$

Alphatrap

from Pentatrap

$$g_{\text{exp}} = g_{\text{theory}}$$ ☺

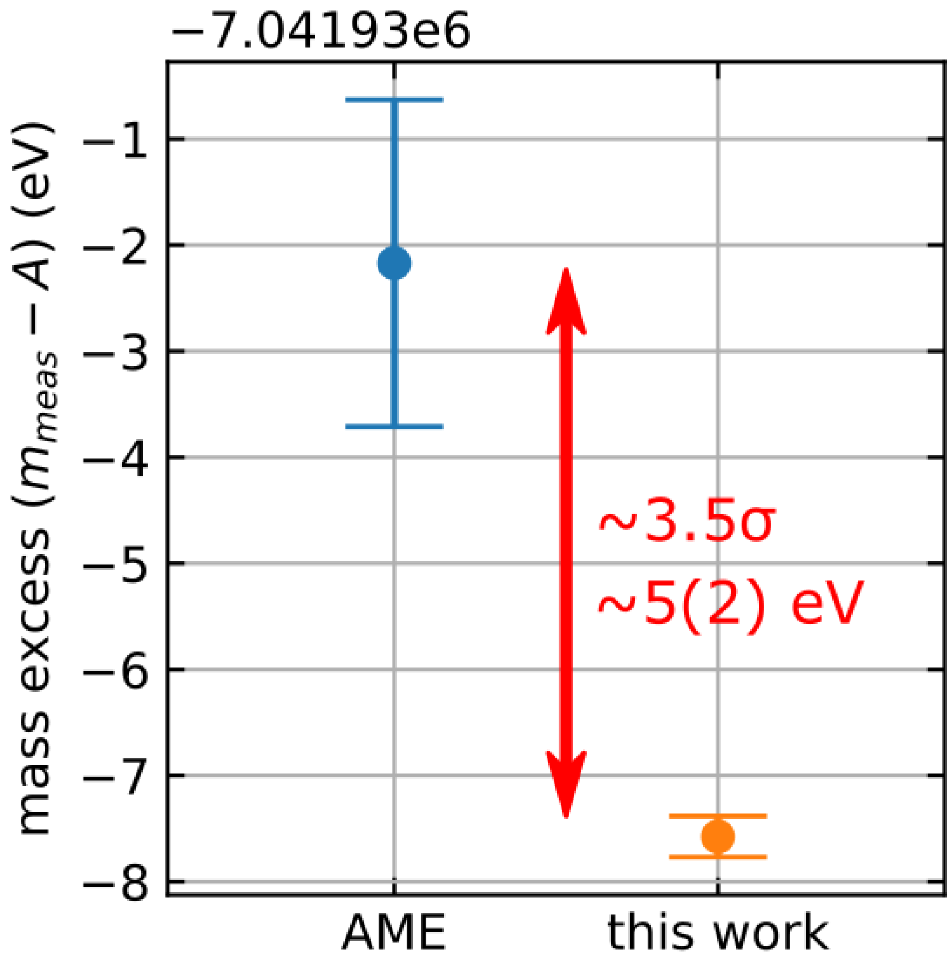

Paper recently accepted at PRL ☺ F. Heisse et. al (2023)

Outline

Pentatrap Lab/Magnet and Trap Tower

- ~~Penning Trap introduction~~
- ~~Pentatrap Setup~~
- ~~Absolute mass measurements (Test of QED)~~
- Isotope chain mass-ratios (search for 5th force)

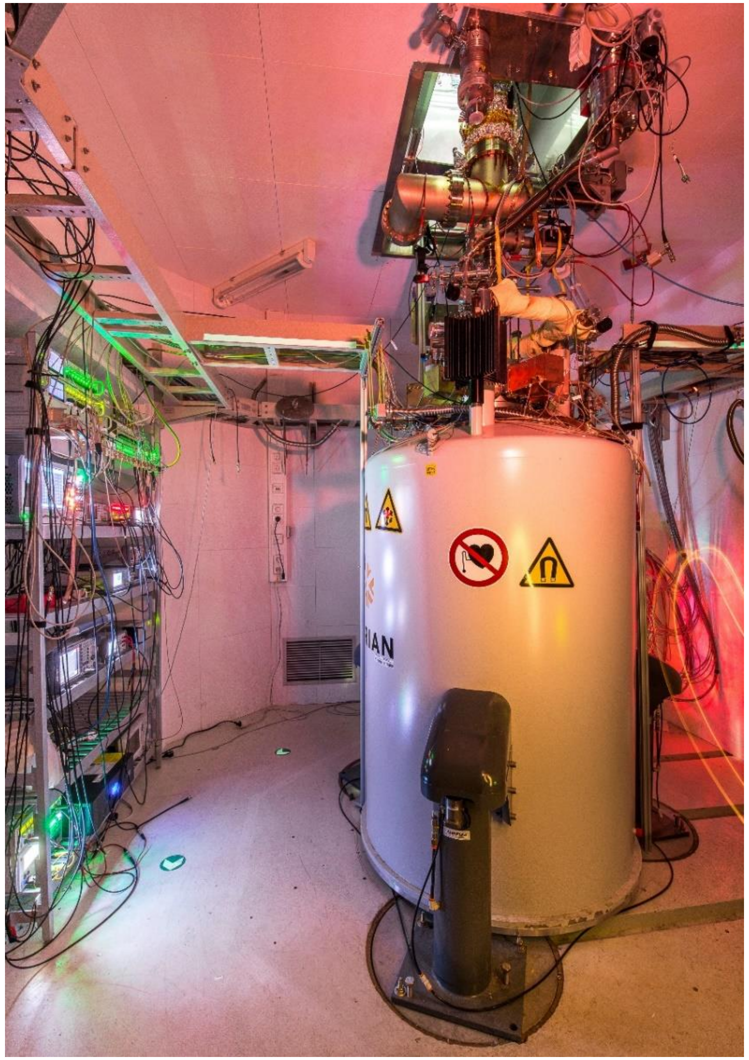

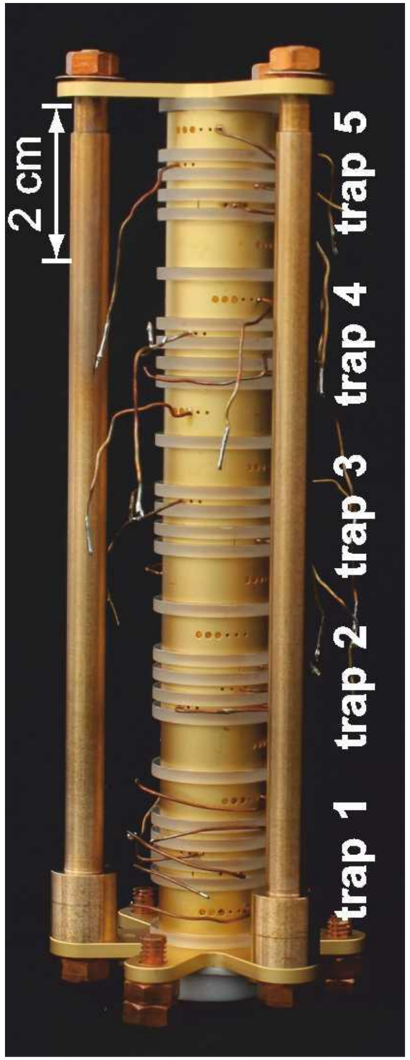

5th force search – Isotope shift King plot analysis

$$\delta R \approx 5 * 10^{-12}$$

strongest systematic uncertainties:

1) dip line shape / fit
2) relativistic shifts

Measured as non-doublets:

- All isotopes at 42+ charge state
- Detection system tuned to match axial and resonator frequency
- No systematics due to B1&C1 (!)

Improved mass-ratios by at least factor of 20 compared to AME

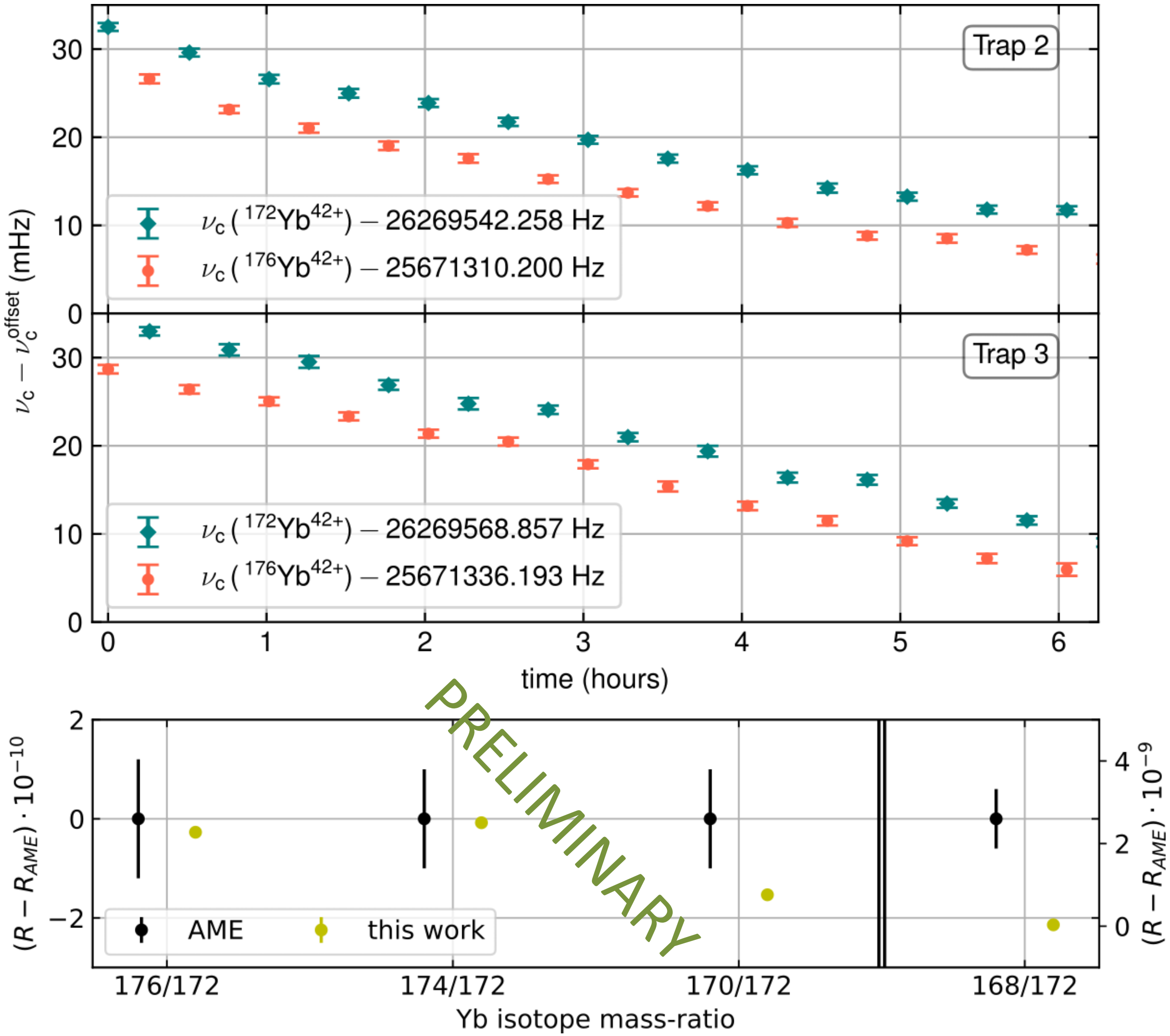

5th force search – Isotope shift King plot analysis

King plot:

With spectroscopy data (1 Hz precision) from the group of Tanja Mehlstaeubler, PhD student Chih-Han Yeh (PTB Braunschweig, Germany)

Further Analysis (limits on New Physics) is still ongoing (Julian Berengut)

Problems:

- Nuclear deformation effects are dominant source of non-linearity -> Group of Achim Schwenk involved
- Ideally these deformations and their impact on the measured isotope shifts can be calculated based on theory
- The successfull correction would make bounds on new physics possible again.

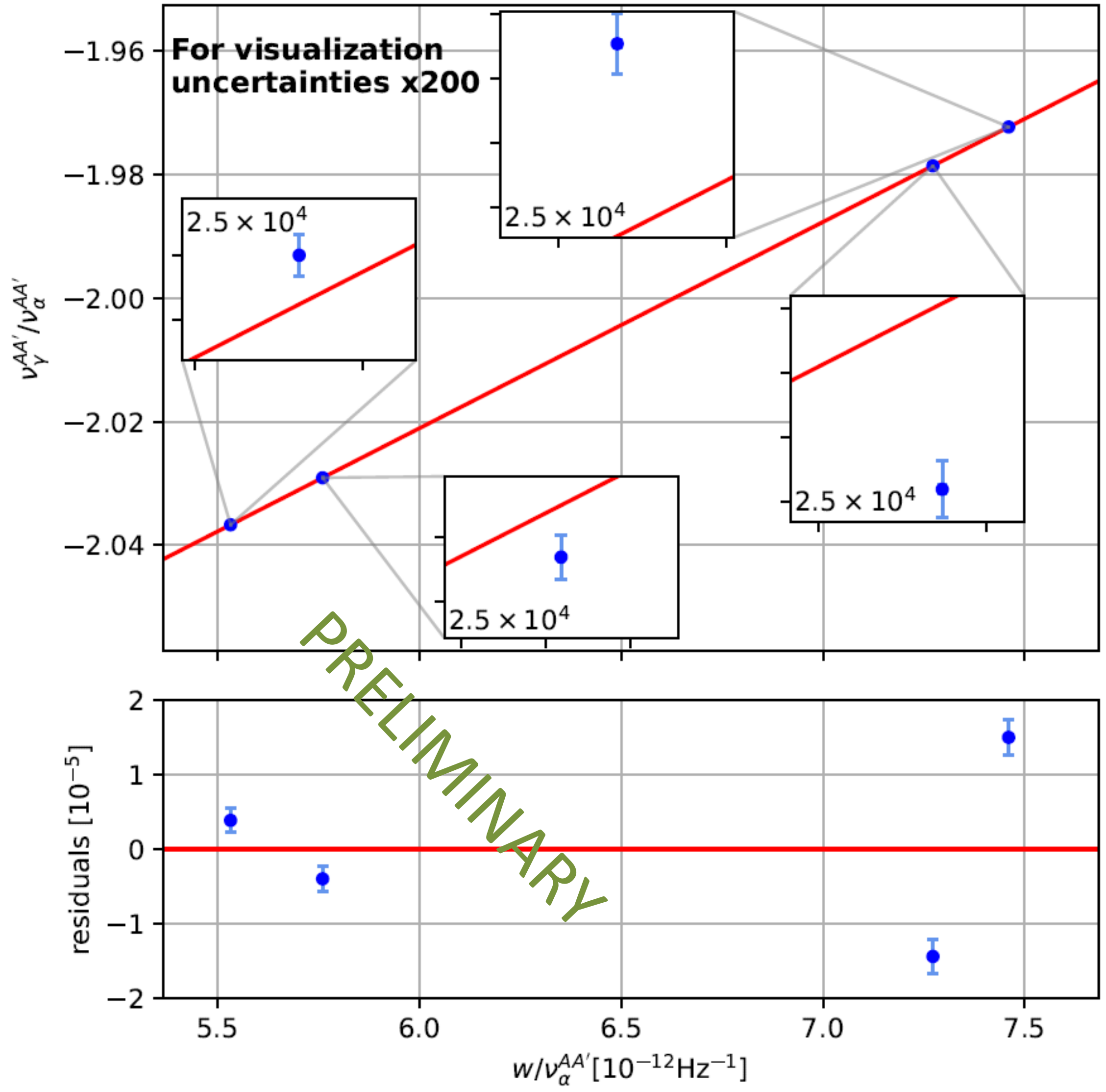

Summary and Outlook

- Pentatrap can perfom few ppt mass-ratio measurements on wide range of stable nuclides
- Kathrin will tell you more about ion production and meta stable states!

- Current limitations are
  - the axial dip lineshape and "on-resonance tuning" (systematics)
  - ion temperature & relativistic shifts (systematics & statistics)
  - Field stabilities (statistics)

Next measurements:

1) Calcium chain for fifth force search

2) Rb and Cs absolute masses, supporting recoil experiments for the determination of the fine structure constant

3) Meta stable states for HCI clocks

Next Upgrades:

1) Feedback cooling to reduce radial amplitudes

2) Phase sensitive axial frequency measurement

3) Equal resonator frequencies in neighboring traps to use same trapping potential source (cancellation?)

MAX-PLANCK-INSTITUT FÜR KERNPHYSIK

Thank you for your attention!

DFG FOR 2202

DFG SFB 1225

IMPRS for Precision Tests of Fundamental Symmetries
INTERNATIONAL MAX PLANCK RESEARCH SCHOOL

European Research Council
Established by the European Commission

ERC AdG 832848 - FunI

Present and former PENTATRAP members:

Christine Böhm, Menno Door, Andreas Dörr, Sergey Eliseev, Lucia Enzmann, Pavel Filianin, Jost Herkenhoff, Daniel Lange, Kathrin Kromer, Marius Müller, Jan Nägele, Yuri N. Novikov, Julia Repp, Alexander Rischka, Christian Roux, Christoph Schweiger, Rima X. Schüssler and Klaus Blaum

BACKUP SLIDES

5th force search – Isotope shift King plot analysis

$$\Delta\nu_i = C_1 \cdot \frac{m_1 - m_2}{m_1 m_2} + C_2 \cdot \Delta\nu_j + \text{[higher–order SM effects + LDM bosons]}$$

$$\nu_i(\text{isotope}_1) - \nu_i(\text{isotope}_2) \equiv \Delta\nu_i$$

King‘s plot

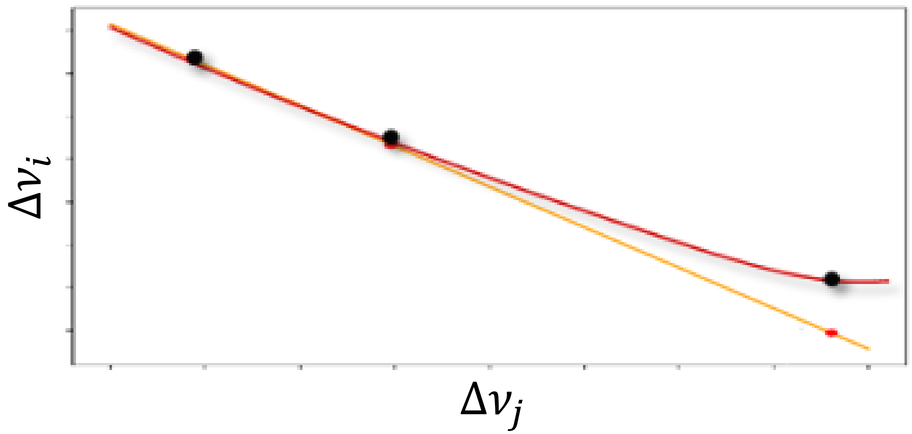

5th force search – Isotope shift King plot analysis

$$\Delta\nu_i = C_1 \cdot \frac{m_1 - m_2}{m_1 m_2} + C_2 \cdot \Delta\nu_j + \text{[higher–order SM effects + LDM bosons]}$$

$$\nu_i(\text{isotope}_1) - \nu_i(\text{isotope}_2) \equiv \Delta\nu_i$$

King's plot

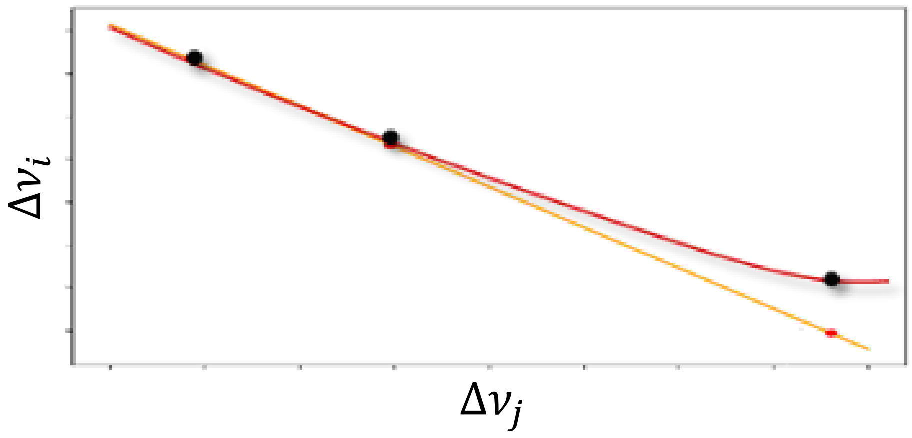

one needs elements with many even-even isotopes
and quadrupole (narrow optical) transitions:

^{168,170,172,174,176}Yb	$^2S_{1/2} \leftrightarrow {}^2D_{5/2}$ (411 nm) $^2S_{1/2} \leftrightarrow {}^2D_{3/2}$ (436 nm)	I. Counts et al., PRL 125, 123002 (2020)
^{40,42,44,46,48}Ca	$4s^2S_{1/2} \leftrightarrow 3d^2D_{5/2}$ (729 nm) $4s^2S_{1/2} \leftrightarrow 3d^2D_{3/2}$ (732 nm)	C. Solaro et al., PRL 125, 123003 (2020) F.W. Knollmann et al., PRA 100, 022514 (2019)
^{84,86,88,90}Sr	$5S_{1/2} - 4D_{5/2}$ $1S_0 - 3P_1$, $1S_0 - 3P_0$	T. Manowitz et al., PRL 123, 203001 (2019) H. Miyake et al., PRR 1, 033113 (2019)

^{142,144,146,148,150}Nd	^{130,132,134,136,138}Ba
N. Bhatt et al., ArXiv 2002.08290	P. Imgram et al., PRA 99, 012511 (2019)

5th force search – Isotope shift King plot analysis

$$\Delta\nu_i = C_1 \cdot \frac{m_1 - m_2}{m_1 m_2} + C_2 \cdot \Delta\nu_j + \text{[higher–order SM effects + LDM bosons]}$$

$$\nu_i(\text{isotope}_1) - \nu_i(\text{isotope}_2) \equiv \Delta\nu_i$$

King's plot

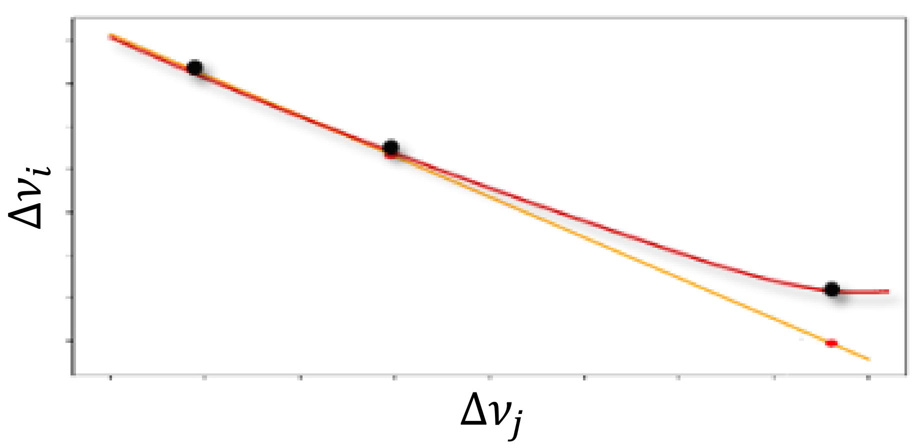

one needs elements with many even-even isotopes
and quadrupole (narrow optical) transitions:

^{168,170,172,174,176}Yb	$^2S_{1/2} \leftrightarrow {}^2D_{5/2}$ (411 nm) $^2S_{1/2} \leftrightarrow {}^2D_{3/2}$ (436 nm)	I. Counts et al., PRL 125, 123002 (2020)
^{40,42,44,46,48}Ca	$4s^2S_{1/2} \leftrightarrow 3d^2D_{5/2}$ (729 nm) $4s^2S_{1/2} \leftrightarrow 3d^2D_{3/2}$ (732 nm)	C. Solaro et al., PRL 125, 123003 (2020) F.W. Knollmann et al., PRA 100, 022514 (2019)
^{84,86,88,90}Sr	$5S_{1/2} - 4D_{5/2}$ $1S_0 - 3P_1$, $1S_0 - 3P_0$	T. Manowitz et al., PRL 123, 203001 (2019) H. Miyake et al., PRR 1, 033113 (2019)

^{142,144,146,148,150}Nd	^{130,132,134,136,138}Ba
N. Bhatt et al., ArXiv 2002.08290	P. Imgram et al., PRA 99, 012511 (2019)

FUTURE of Yb:

$$\delta(\Delta\nu_i) \approx 10 \text{ mHz}$$

$$\delta\left(\frac{m_1}{m_2}\right) \approx 5 \cdot 10^{-12}$$

5th force search – Isotope shift King plot analysis

^{187}Re/ ^{187}Os, ^{187m}Re/ ^{187g}Re, ^{187m}Os/ ^{187g}Os, ^{163}Ho/ ^{163}Dy, ^{12}C/ ^{20}Ne – mass or *m/q* doublets !!!

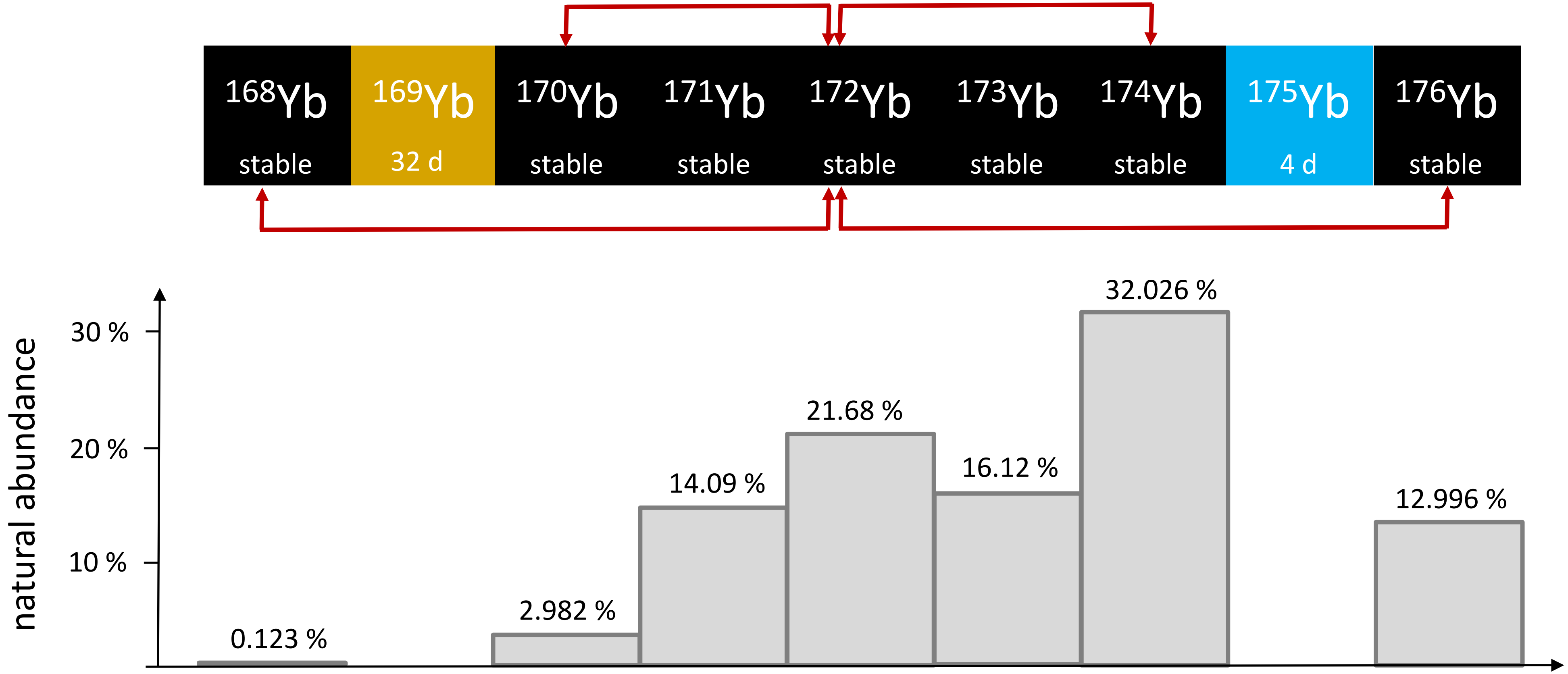

Independent analysis methods

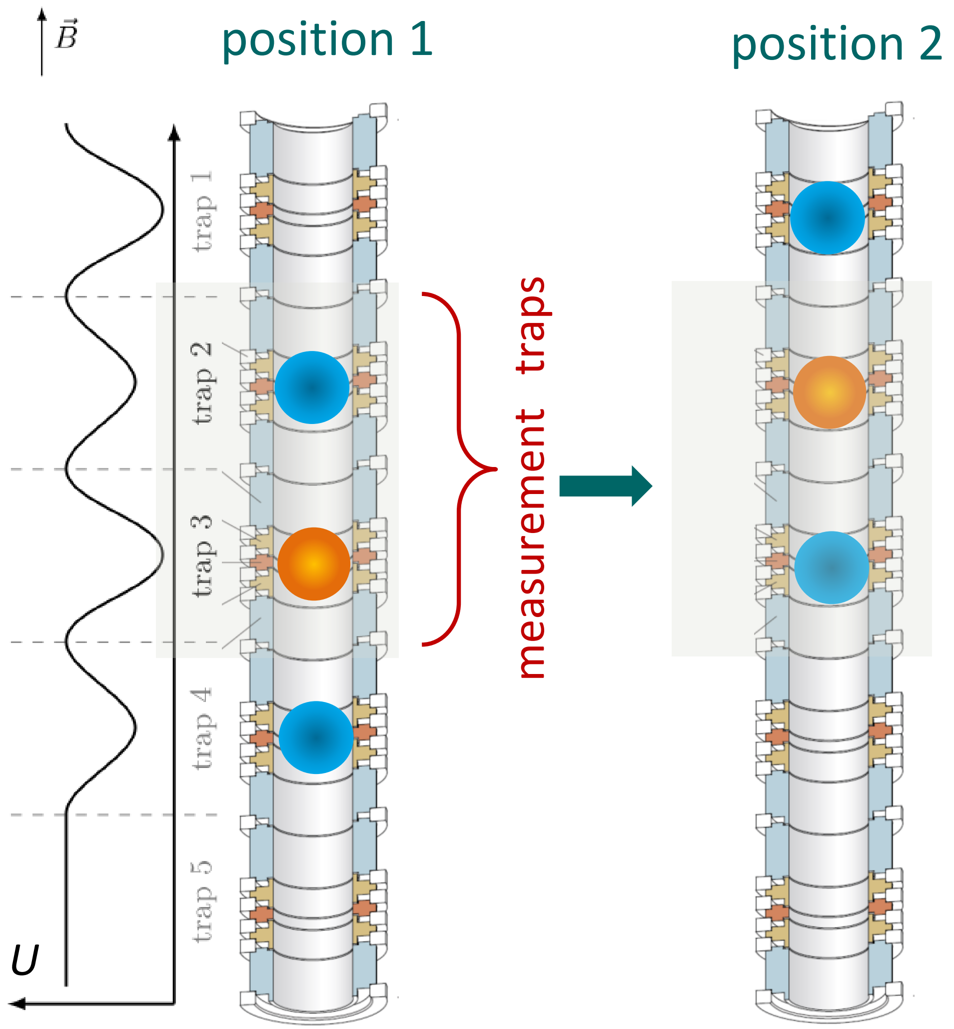

various data analysis methods:

- interpolation
- polynomial
- cancelation
- polycancel

⬇

reliability of results

^{A}Yb /$^{A'}$Yb issues with same-charge state measurements:

- Difference in axial frequency is huge! Up to 8 kHz! But axial frequency has to match detection system
  → trap depth has to be adjusted for each ion

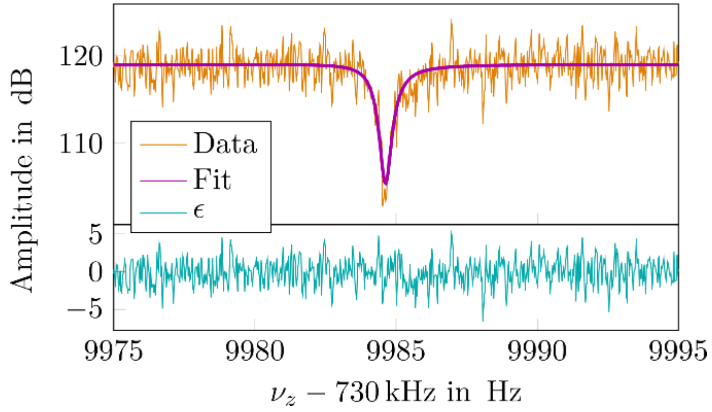

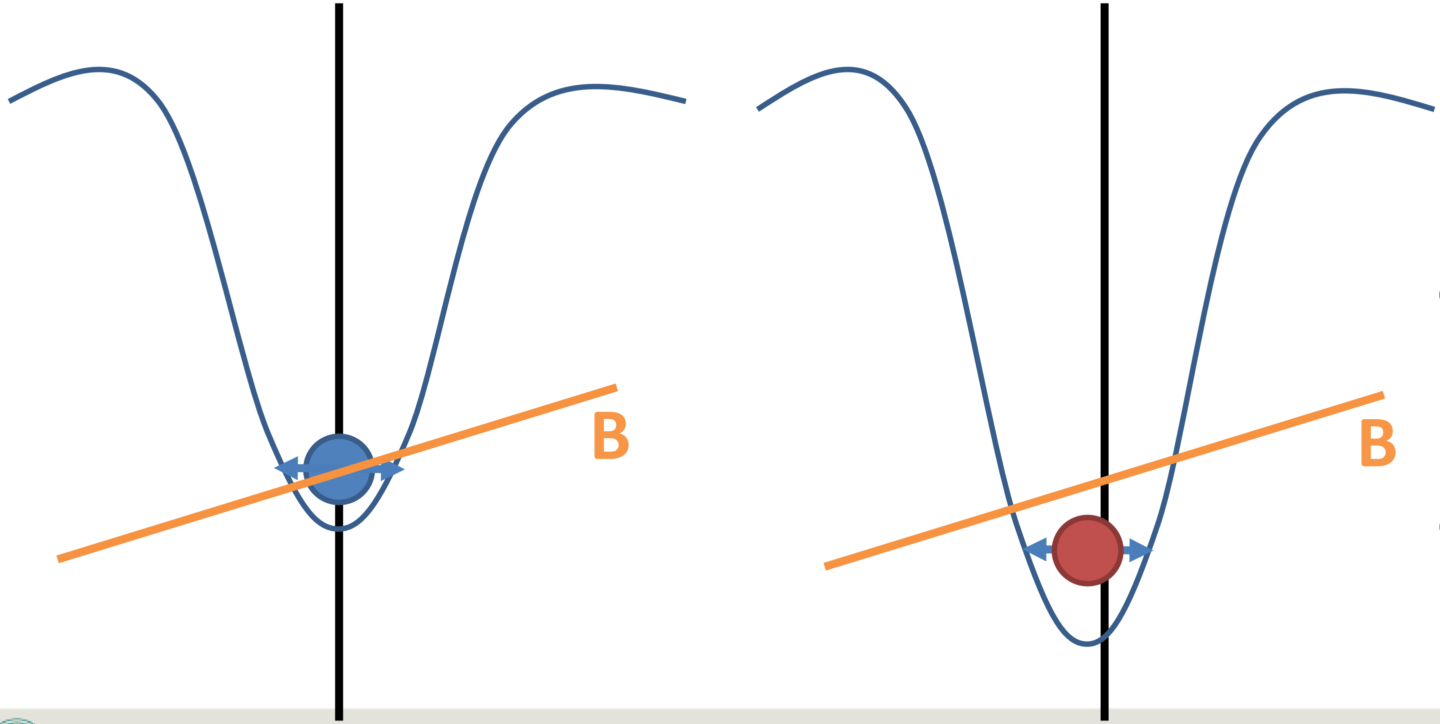

Problem:

Potential not perfectly symmetric
→ depth change = ion mean position changes

Magnetic field not perfectly homogeneous: effective magnetic field changes

$$\boxed{R = \frac{\omega_c^A}{\omega_c^B} = \frac{q^A m^B}{q^B m^A}\frac{B^A}{B^B}}$$

^{A}Yb /$^{A'}$Yb issues with same-charge state measurements:

- Difference in axial frequency is huge! Up to 8 kHz! But axial frequency has to match detection system
  → trap depth has to

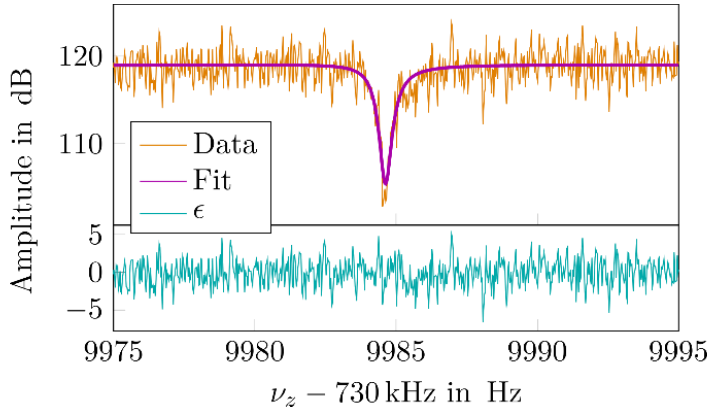

Huge systematic effect on the mass ratio result…
Not feasable

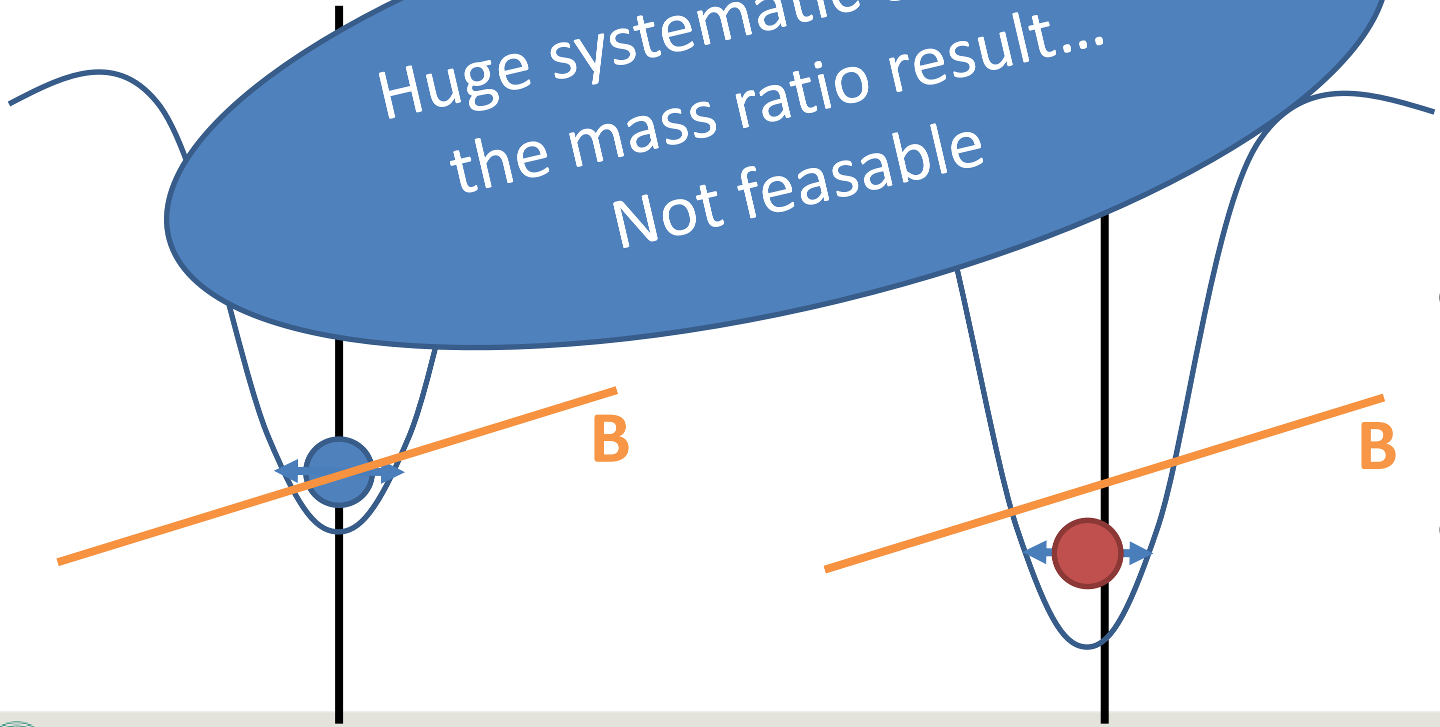

Problem:

Potential not perfectly symmetric
→ depth change = ion mean position changes

Magnetic field not perfectly homogeneous: effective magnetic field changes

$$\boxed{R = \frac{\omega_c^A}{\omega_c^B} = \frac{q^A m^B}{q^B m^A}\frac{B^A}{B^B}}$$

^{A}Yb /$^{A'}$Yb issues with same-charge state measurements:

- Difference in axial frequency is huge! Up to 8 kHz! But axial frequency has to match detection system
  → trap depth has to be adjusted for each ion

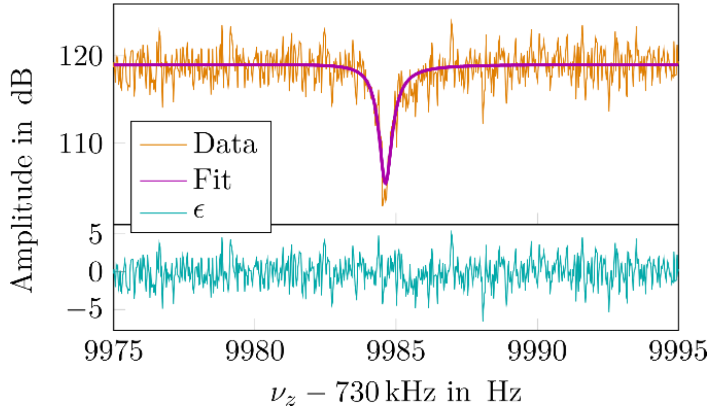

- Solution: VariCap (variable capacitance) to tune detection system instead of trap potential

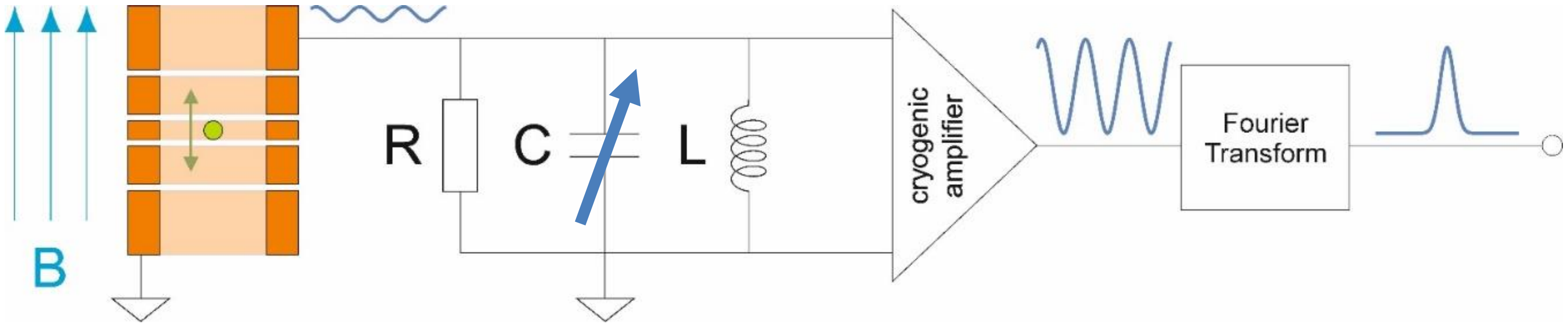

Varactor Upgrade

Varactor control was added for all 3 center traps resonators

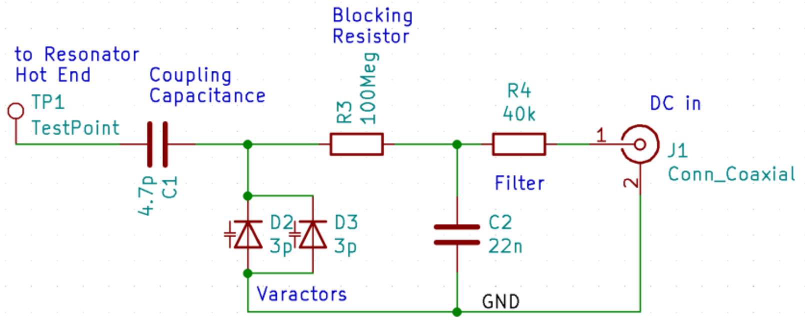

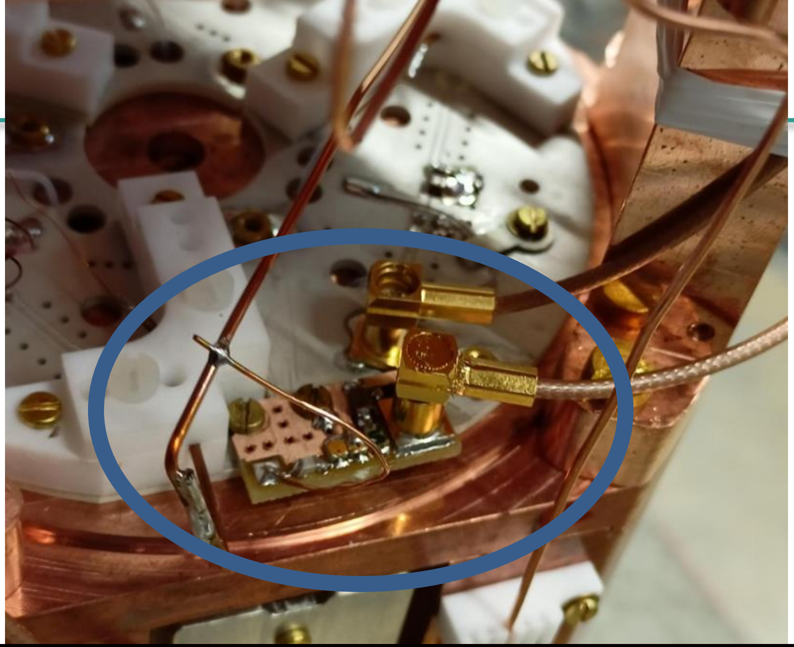

Resonator now tunable (12 kHz roughly)

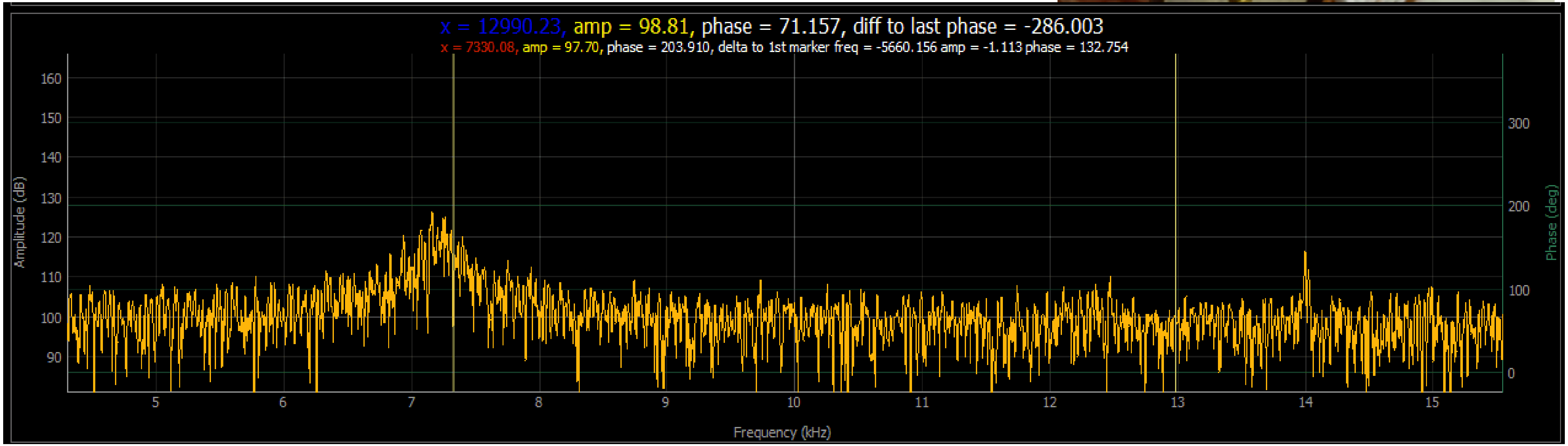

IS spectroscopy

Counts, I. *et. al.*, arXiv:2004.11383v2

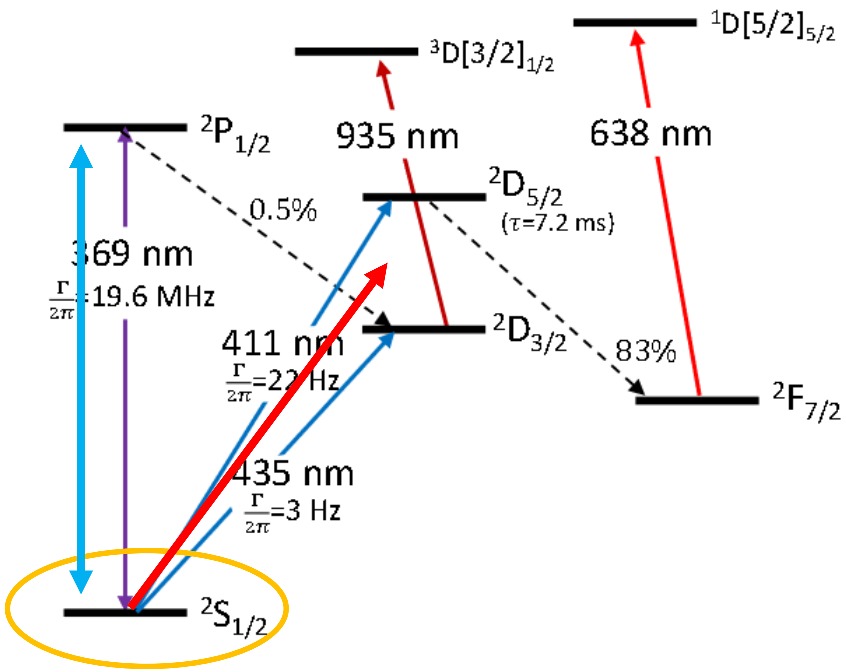

FIG. S1. Partial Yb$^+$ level diagram.

- single Yb+ ion trapped 135μm above the a lithographic microchip surface Paul trap
- The transitions at 411 nm (6s^2 S1/2 → 5d^2 D5/2; Γ/(2π) = 22 Hz) and 436 nm (6s^2 S1/2 → 5d^2 D3/2; Γ/(2π) = 3 Hz) are probed with a Ti:Sapphire laser, tuned to 822 nm and 871 nm, respectively
- The readout of the state is carried out via an electron-shelving scheme (dark state detection) – we covered this not long ago in the Journal Club, here a small recap:

1. Ions in the ground state S1/2 are detected via fluorescence during the cooling with 369 nm light.
2. If the ion is fluorescing before a probe pulse and no longer fluorescing afterwards, the ion is said to have completed a quantum jump.
3. Otherwise, the ion failed to quantum jump (or, if there was no fluorescence before the probe pulse, the ion failed to be initialized).
4. By dividing the number of quantum jumps by the total number of successful initialization, we can measure a probability of excitation as a function of frequency.

~ 400 Hz precision on the measured transitions
@ 2 GHz IS, relative ~ 2e-7

IS spectroscopy

Counts, I. *et. al.*, arXiv:2004.11383v2

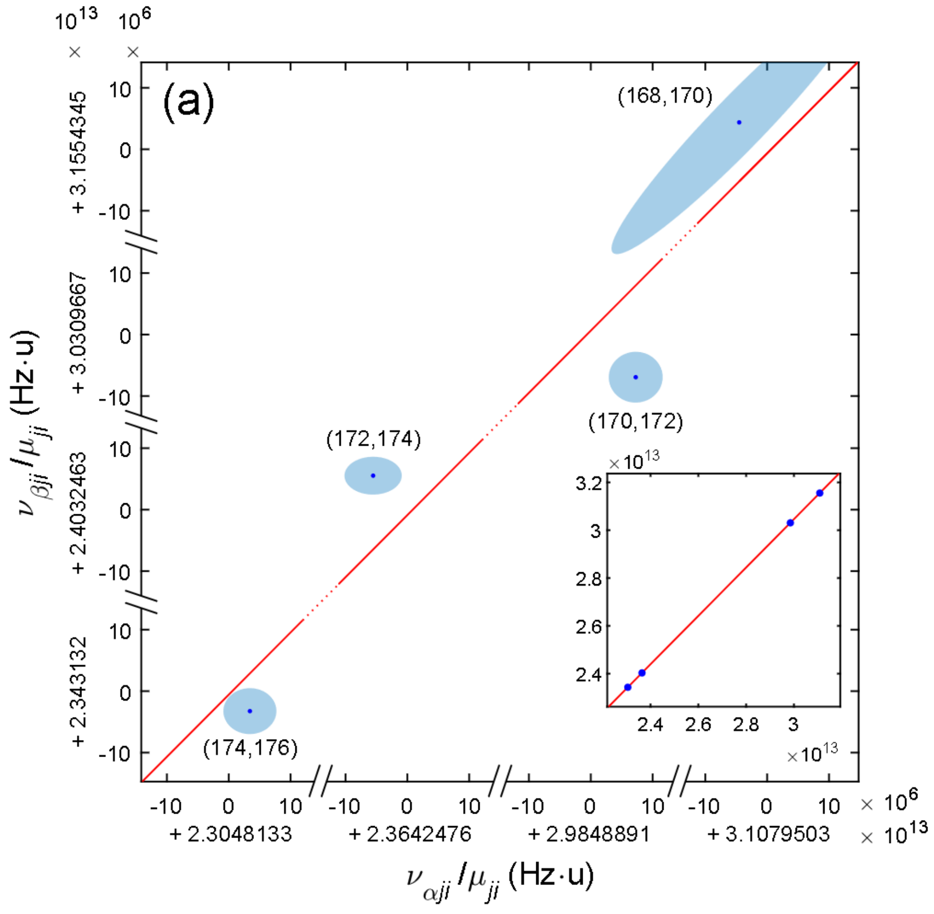

- single Yb+ ion trapped 135μm above the a lithographic microchip surface Paul trap
- The transitions at 411 nm (6s^2 S1/2 → 5d^2 D5/2; Γ/(2π) = 22 Hz) and 436 nm (6s^2 S1/2 → 5d^2 D3/2; Γ/(2π) = 3 Hz) are probed with a Ti:Sapphire laser, tuned to 822 nm and 871 nm, respectively
- The readout of the state is carried out via an electron-shelving scheme (dark state detection) – we covered this not long ago in the Journal Club, here a small recap:

1. Ions in the ground state S1/2 are detected via fluorescence during the cooling with 369 nm light.
2. If the ion is fluorescing before a probe pulse and no longer fluorescing afterwards, the ion is said to have completed a quantum jump.
3. Otherwise, the ion failed to quantum jump (or, if there was no fluorescence before the probe pulse, the ion failed to be initialized).
4. By dividing the number of quantum jumps by the total number of successful initialization, we can measure a probability of excitation as a function of frequency.

~ 400 Hz precision on the measured transitions
@ 2 GHz IS, relative ~ 2e-7

IS spectroscopy (future)

Manovitz, T. et al. Phys. Rev. Lett. **123** (2019) 203001

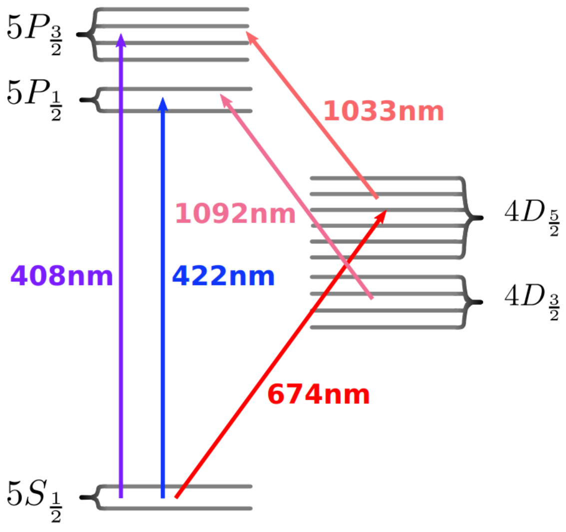

Figure 6.1: $^{88}Sr^{+}$ energy levels diagram

- Two isotope ion crystal of Sr86 and Sr88 in Paul trap
- Also state read out (fluorescence, state preparation, cooling) via an electron-shelving scheme (dark state detection) but using bichromatic laser fields resonant to the relevant transitions in both isotopes.
- The 5S1/2 → 4D5/2 transition is driven by a narrow (~20 Hz) linewidth laser, splitted into different AO frequency shifters that bridge the ~570 MHz IS gap. The two beams are recombined and sent through another AO frequency shifter for common frequency control
- Ions are prepared in entangled state $|\psi_i\rangle = \frac{1}{\sqrt{2}}\left(|g_m e_n\rangle + e^{i\phi_0}|e_m g_n\rangle\right)$.
- The energy difference between the two states in this superposition is exactly the isotope shift times the Planck constant. Therefore, during free evolution for time τ, these states will acquire a relative

$$|\psi_\tau\rangle = \frac{1}{\sqrt{2}}\left(|g_m e_n\rangle + e^{i\phi_0 - i\delta\nu^i_{nm}\tau}|e_m g_n\rangle\right)$$

IS spectroscopy (future)

Manovitz, T. et al. Phys. Rev. Lett. **123** (2019) 203001

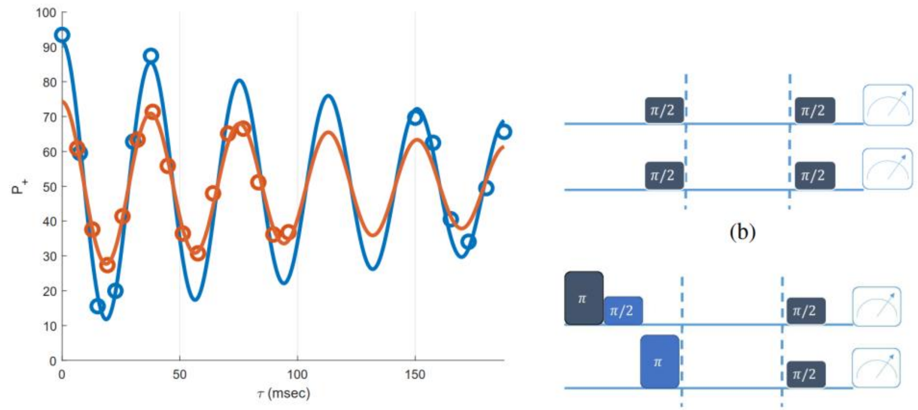

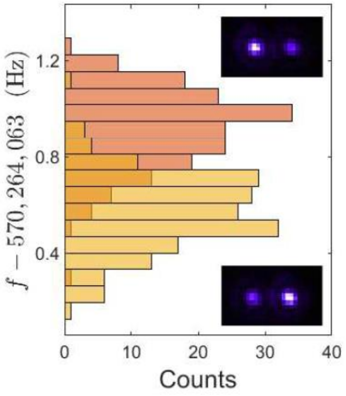

Reaching ~ 10 mHz precision directly on IS(!)
@ 570 MHz, relative ~ 1E-11

- Ions are prepared in entangled state $$|\psi_i\rangle = \frac{1}{\sqrt{2}}\left(|g_m e_n\rangle + e^{i\phi_0}|e_m g_n\rangle\right).$$
- The energy difference between the two states in this superposition is exactly the isotope shift times the Planck constant. Therefore, during free evolution for time τ, these states will acquire a relative

$$|\psi_\tau\rangle = \frac{1}{\sqrt{2}}\left(|g_m e_n\rangle + e^{i\phi_0 - i\delta\nu^i_{nm}\tau}|e_m g_n\rangle\right)$$

- The superposition phase is estimated by performing a parity measurement. Two π/2 pulses are applied, each at the carrier frequency of one of the isotopes. The resulting populations will obey the relation

$$p_{ee} + p_{gg} - (p_{eg} + p_{ge}) = \cos\left(\phi_0 + \delta\nu^i_{nm}\tau - (\varphi_m - \varphi_n)\right)$$

$$= \cos\left(\phi_0 + (\delta\nu^i_{nm} - \delta f_{nm})\tau - (\phi_m - \phi_n)\right)$$

- The parity signal will oscillate in time at the detuning of the two fields' frequency difference, which can be dictated by an RF source, with respect to the isotope shift. Laser phase-noise is cancelled since it is common to both addressing fields.

Mass situation

Nuclide	Current mass precision (AME2016) $\delta m/m$	Labs performing spectroscopy measurements of the IS
Ca40	**5.51e-10**	PTB (Germany) IQOQI (Austria)
Ca42	**3.79e-09**	
Ca44	**7.92e-09**	
Ca46	**5.22e-08**	
Ca48	**2.15e-09**	
Sr84	**1.59e-08**	Weizmann Institute (Israel) RIKEN (Japan)
Sr86	6.53e-11	
Sr88	6.81e-11	
Sr90	**2.54e-08**	
Yb168	**7.63e-09**	Weizmann Institute (Israel) NIST (USA)
Yb170	6.47e-11	
Yb172	8.14e-11	
Yb174	6.32e-11	
Yb176	8.53e-11	

Better value JYFLTRAP 2020

Needed relative precision compared to IS precision, a factor of roughly: $\dfrac{m_A}{m_{A_0} - m_A}$	Current IS precision	Needed mass precision
48/8 = 6	~ 1e-08	~ 2e-09
88/4 = 22	~ /	
176/8 = 22	~ 1e-07	~ 5e-09

King Plot – vector space

I. VISUALIZING THE VECTOR SPACE

In the main text we define the following vectors in the A' vector space

$$\overrightarrow{m\nu}_i \equiv \left(m\nu_i^{AA'_1}, m\nu_i^{AA'_2}, m\nu_i^{AA'_3}\right) , \quad \text{(S1)}$$

$$\overrightarrow{m\delta\langle r^2\rangle} \equiv \left(\langle r^2\rangle_{AA'_1}/\mu_{AA'_1}, \langle r^2\rangle_{AA'_2}/\mu_{AA'_2}, \langle r^2\rangle_{AA'_3}/\mu_{AA'_3}\right) , \quad \text{(S2)}$$

$$\overrightarrow{m\mu} \equiv (1,1,1) . \quad \text{(S3)}$$

As long as $\overrightarrow{m\nu}_{1,2}$ are spanned by $\overrightarrow{m\mu}$ and $\overrightarrow{m\delta\langle r^2\rangle}$, the resulting King plot will be linear. In Fig. S1, we illustrate the vector space of the various components related to isotope shifts that leads to the nonlinearites. The NP contribution to IS, $\alpha_{\rm NP} X_i \vec{h}$, may lift the IS vectors from the $(\overrightarrow{m\mu}, \overrightarrow{m\delta\langle r^2\rangle})$ plane, resulting in a nonlinear King plot. Fig. S2 illustrates a nonlinear King plot, where the area of the triangle corresponds to the NL of Eq. (6).

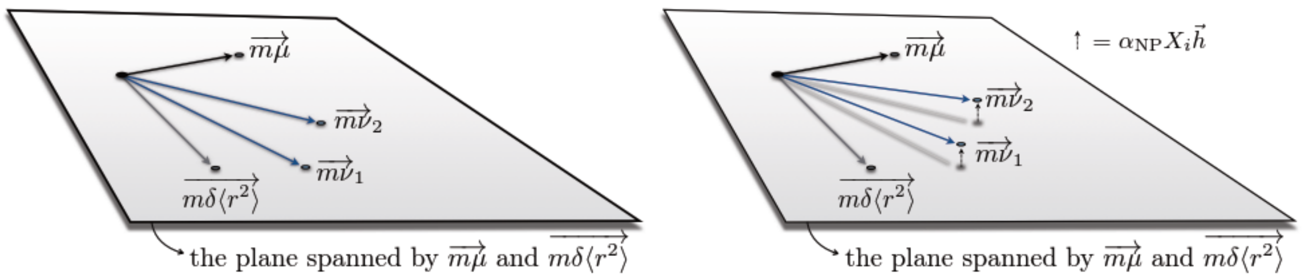

FIG. S1: Left: A cartoon of the prediction of factorization, Eq. (5) in vector language. All of the isotope shift measurements (which are here three dimensional vectors $\overrightarrow{m\nu}_{1,2}$) lie in the plane that is spanned by $\overrightarrow{m\mu}$ and $\overrightarrow{m\delta\langle r^2\rangle}$. This coplanarity can be tested by measuring whether $\overrightarrow{m\nu}_1$, $\overrightarrow{m\nu}_2$ and $\overrightarrow{m\mu}$ are coplanar. Right: In the presence of new physics the isotope shift get a contribution which can point out of the plane. A new long range force can spoil the coplanarity of $\overrightarrow{m\nu}_1$, $\overrightarrow{m\nu}_2$ and $\overrightarrow{m\mu}$.

Reminder…

$$m\nu_i^{A_0A} = \frac{\nu_i^{A_0A}}{\mu_{A_0A}} = K_i + \frac{F_i}{\mu_{A_0A}}\,\delta\langle r^2\rangle_{A_0A}$$

$$m\nu_2^{A_0A} = K_{21} + F_{21} m\nu_1^{A_0A}$$

with $F_{21} = F_2/F_1$, *and* $K_{21} = K_2 - F_{21}K_1$

$$\overrightarrow{m\nu}_i = K_i\,\overrightarrow{m\mu} + F_i\,\overrightarrow{m\delta\langle r^2\rangle}.$$

$$\overrightarrow{m\nu}_2 = K_{21}\overrightarrow{m\mu} + F_{21}\overrightarrow{m\nu}_1$$

Nonlinearity?

$$\mathrm{NL} = \frac{1}{2}\left|(\overrightarrow{m\nu}_1 \times \overrightarrow{m\nu}_2)\cdot\overrightarrow{m\mu}\right| . \quad >$$

$$\sigma_{\rm NL} = \sqrt{\Sigma_k(\partial \mathrm{NL}/\partial \mathcal{O}_k)^2\sigma_k^2}$$

(squared error of all measured values)

Berengut, J. *et. al.*, Phys. Rev. Lett. **120** (2018) 091801

Non-linearities

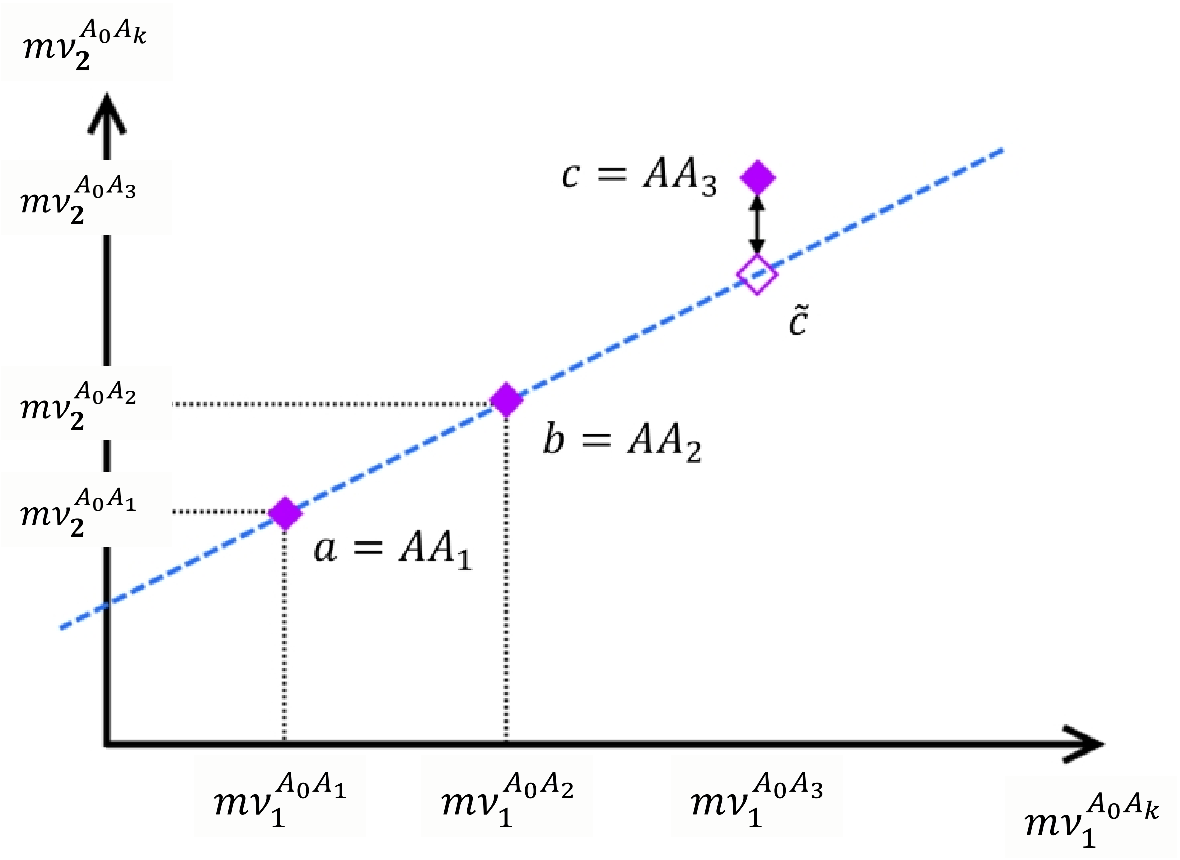

Other sources than new physics: The formular for the IS is an approximation:

$$\nu_i^{AA'} = K_i\,\mu_{AA'} + F_i\,\delta\langle r^2\rangle_{AA'} + \alpha_{NP}X_i\gamma_{AA'}$$

Only valid at leading order of variation of the nuclear mass and charge distribution, expansion needed:

$K_i \rightarrow K_i^{A_0A}$ and $F_i \rightarrow F_i^{A_0A}$

This breaks linearity (now isotope depended)!

Calculating these nuclear effects theoretically is challenging… and with higher precision in the experimental input data, these effect will dominate the linearity test…. more later…

Effects can be parametrized:

$$\nu_i^{AA'} = K_i\,\mu_{AA'} + F_i\,\delta\langle r^2\rangle_{AA'} + \sum_{l=2}^{inf} F_{il}\lambda_{l,A_0A}$$

λ_{l,A_0A}: independ. nuclear param., F_{il}: electronic const.

No-mass King analysis

Uses third transition to remove the mass shift parameters

Two transitions, e.g. i={1,2}, are used to extract the mass and field shift nuclear parameters

$$\nu_i^{A_0 A} = K_i\, \mu_{A_0 A} + F_i\, \delta\langle r^2\rangle_{A_0 A} + \alpha_{NP} X_i \gamma_{A_0 A}$$

Third transition uses nuclear parameters in theory predictions

$$\nu_3^{A_0 A} = f_3^{\alpha}\, \nu_\alpha^{A_0 A} + \alpha_{NP} (X_3 - f_3^{\alpha} X_\alpha)\, \gamma_{A_0 A}$$

Also this linearity by itself can be tested without theory input

No-mass King analysis

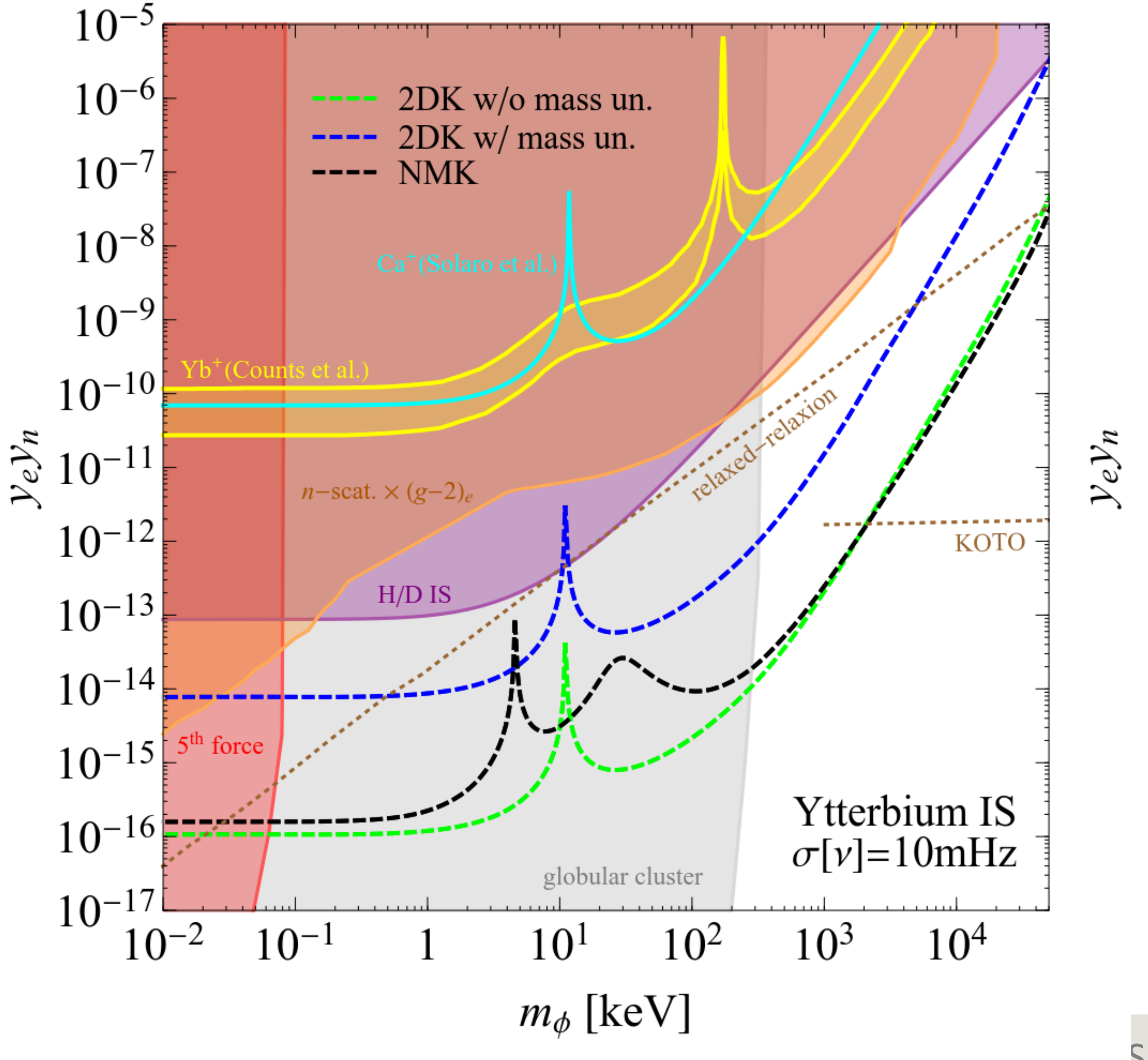

Uses third transition to remove the mass shift parameters

$$\nu_i^{A_0 A} = K_i\, \mu_{A_0 A} + F_i\, \delta\langle r^2\rangle_{A_0 A} + \alpha_{NP} X_i \gamma_{A_0 A}$$

$$\nu_3^{A_0 A} = f_3^{\alpha}\, \nu_\alpha^{A_0 A} + \alpha_{NP}(X_3 - f_3^{\alpha} X_\alpha)\, \gamma_{A_0 A}$$

Generalized King analysis (GK)

Basically the same as the no-mass analysis: using additional transitions to exchange additional electronic and nuclear parameters by IS measurement data

At least m-1 transitions needed to fix parameters… Reaching this relation:

(Apperently) this generalized King analysis method allows to probe for new physics even though the typical King linearity is broken. It needs however m+2 isotopes and m-1 transitions…

This is possible for Ytterbium (5 isotopes, 3 transitions)

$$m\nu_i^{AA'} = K_i + \sum_{l=1}^{m-1} F_{il} m\lambda_{l,A_0A} + \alpha_{NP} X_i h_{A_0A}$$

λ_{l,A_0A}: independ. nuclear param., F_{il}: electronic const.

$$m\nu_k^a = [K_k - f_{ki}K_i] + f_{ki} m\nu_i^a + \alpha_{\mathrm{NP}}[X_k - f_{ki}X_i]h_a, \quad (11)$$

Generalized King analysis (GK)

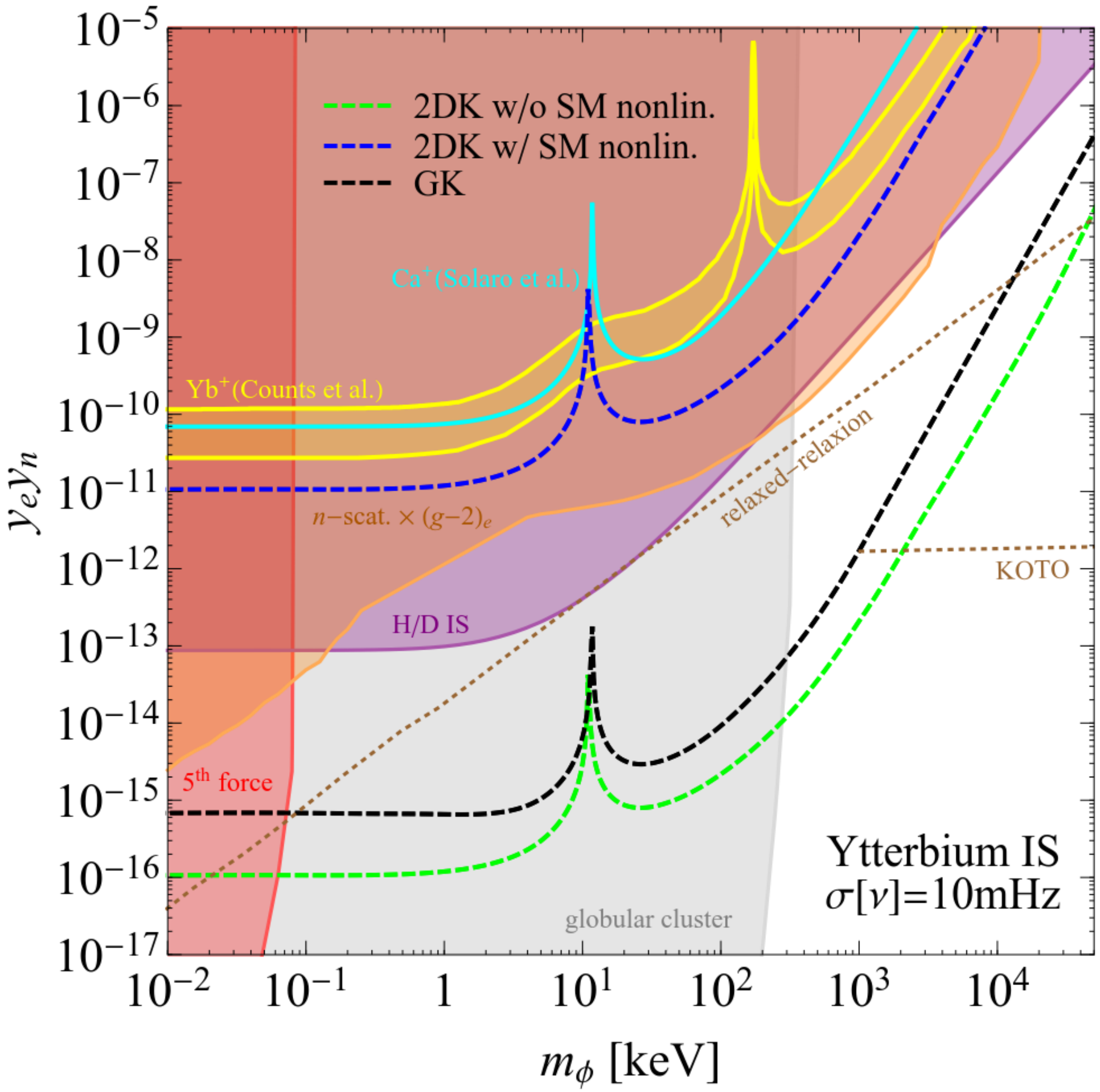

$$m\nu_i^{AA'} = K_i + \sum_{l=1}^{m-1} F_{il}\, m\lambda_{l,A_0A} + \alpha_{NP}\, X_i h_{A_0A}$$

λ_{l,A_0A}: independ. nuclear param., F_{il}: electronic const.

$$m\nu_k^a = [K_k - f_{ki}K_i] + f_{ki}\, m\nu_i^a + \alpha_{\mathrm{NP}}[X_k - f_{ki}X_i]h_a, \quad (11)$$

SM nonlin. = Standard Model non linearities

Phase sensitive measurement PnP: the sequence

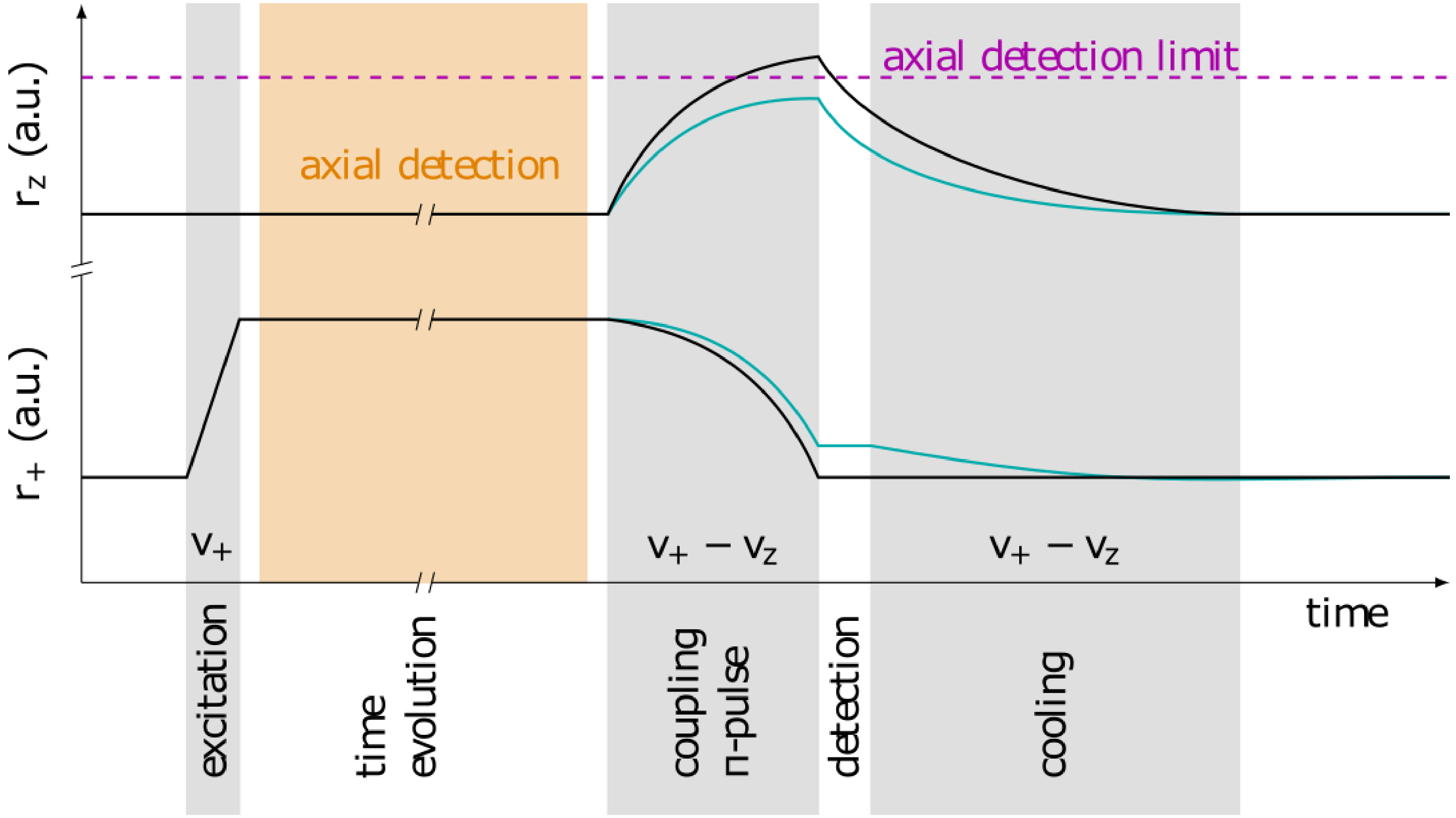

^{20}Ne mass measurement - **Systematics**

Ratio measurements were done at multiple excitaton amplitudes:

No significantly measureable dependence on excitation amplitude

With extrapolation to zero excitation amplitude:

dR ~ 1e-11

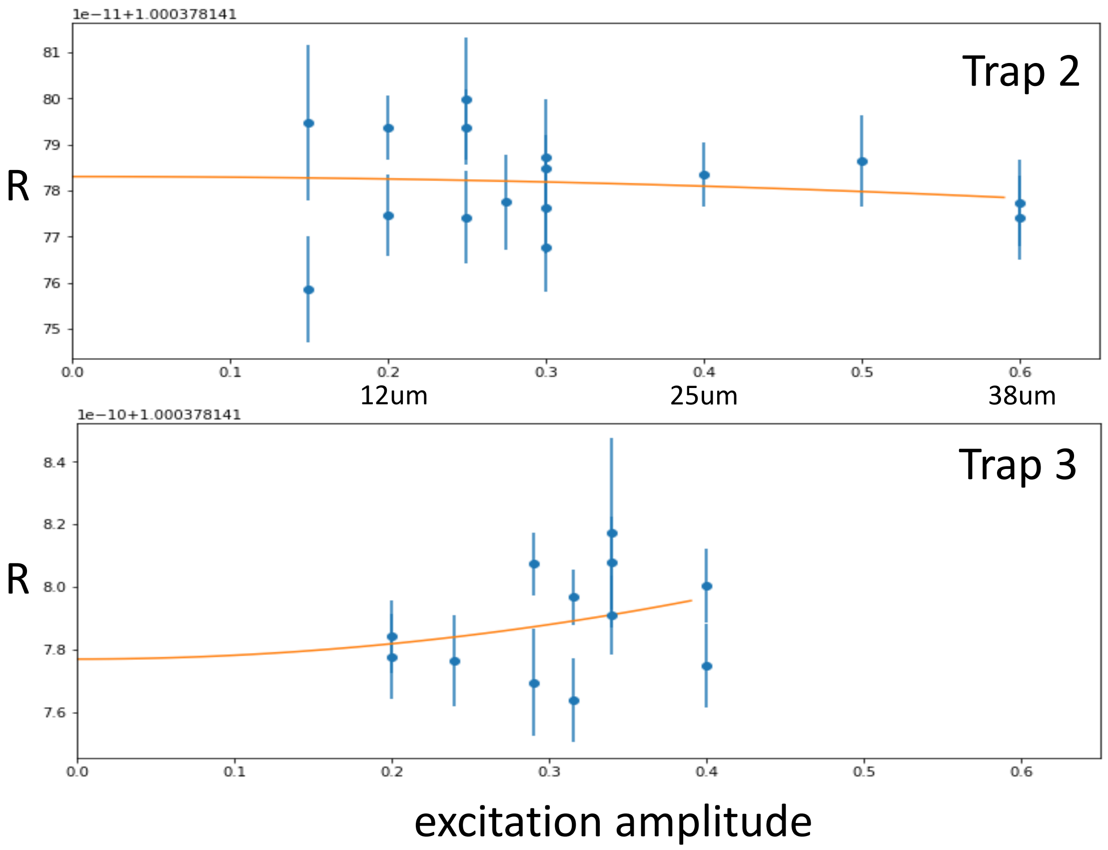

Final measured ratio uncertainty **dR ~ 1e-11**

20-Ne mass measurement

We measure 20Ne10+ against 12C6+. First direct mass measurement with Pentatrap, what is different to higher masses?

Lower masses -> **mass-to-charge-"doubleticity" is often less good**, frequency differences are bigger (in HoDy or for metastables there is no difference in axial frequency and sub Hz difference in cyclotron frequency)

	20Ne10+	**12C6+**	**$\Delta\nu_i$ (Hz)**
ν_+ (Hz)	53792993.89	53772656.43	**20337.46**
ν_z (tuned) (Hz)	736080.7	736080.7	0 (~100 @ same U0)
ν_- (Hz)	5036.09	5038.38	2.29

The difference in ν_+ might(!) result in different excitation radii due to a non-constant transfer function from the RF-generator output to the trap electrodes over the needed frequency range**, e.g. by non-linear filters and/or switches or static noise resonances**.

What would the systematics look like?

More low masses as cross check

We are planning to measure other low masses sooner or later, e.g.:

	$\delta m/m_{AME}$	Group	Year
14N	1.71E-11	MIT / DiFilippo /Pritchard	1995
16O	2.00E-11	UW / van Dyke	2006
28Si	1.97E-11	FSU / Redshaw / Myers	2008

<u>Neon mass measurement showed:</u>

Pentatrap is able to measure low masses.

-> even more candidates to measure!

Systematics are more prominent, better to investigate with low masses.

Discrepancy between AME and our result, more comparisons are needed.

Data Analysis: Cancel Method

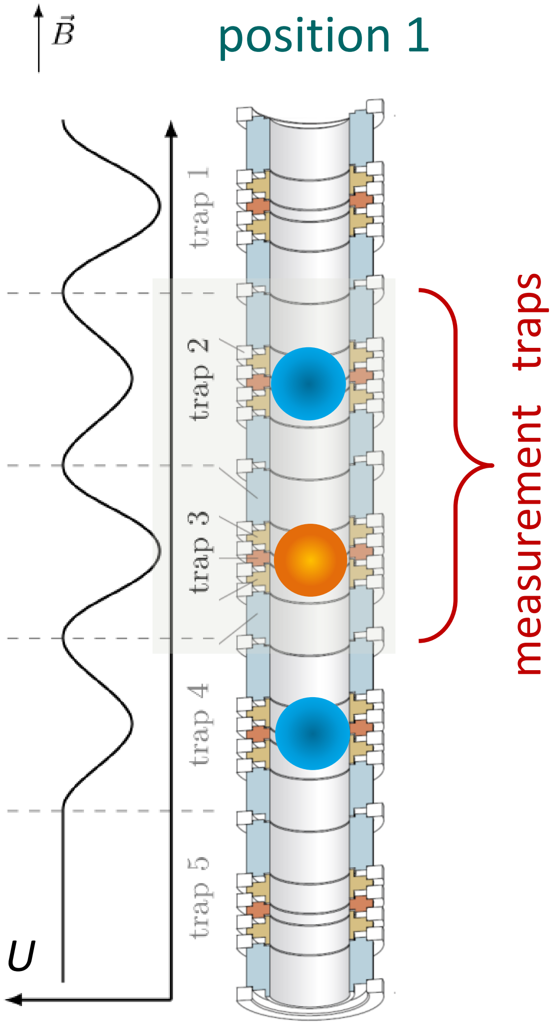

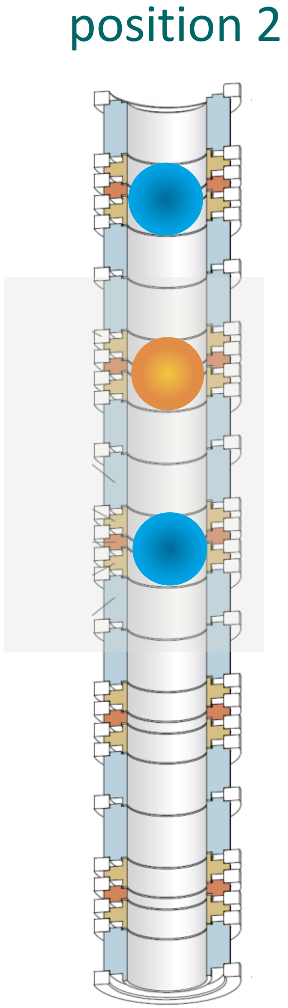

$$R = \sqrt{R(t_1)R(t_2)} = \frac{m_2}{m_1}$$

$$if \ \frac{B_{trap2}}{B_{trap3}} = const$$

$$R(t_1) = \frac{\nu_{ion1}}{\nu_{ion2}}(t_1) = \frac{m_2}{m_1}\frac{B_{trap2}}{B_{trap3}}(t_1)$$

$$R(t_2) = \frac{\nu_{ion1}}{\nu_{ion2}}(t_2) = \frac{m_2}{m_1}\frac{B_{trap3}}{B_{trap2}}(t_2)$$

some photos of traps and axial resonators

trap tower

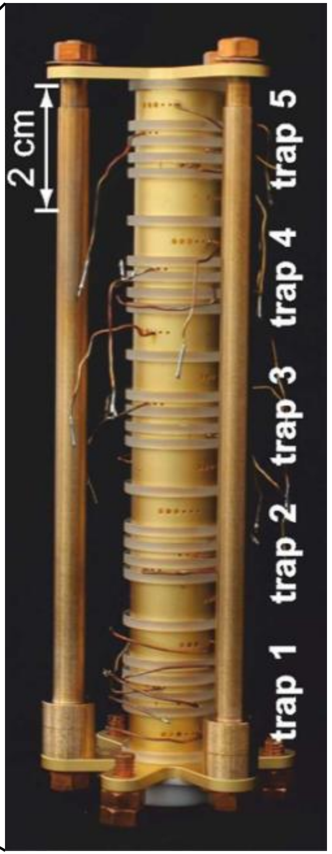

trap electrodes

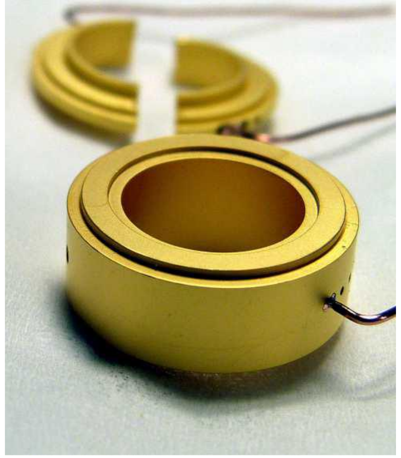

NbTi toroidal coil

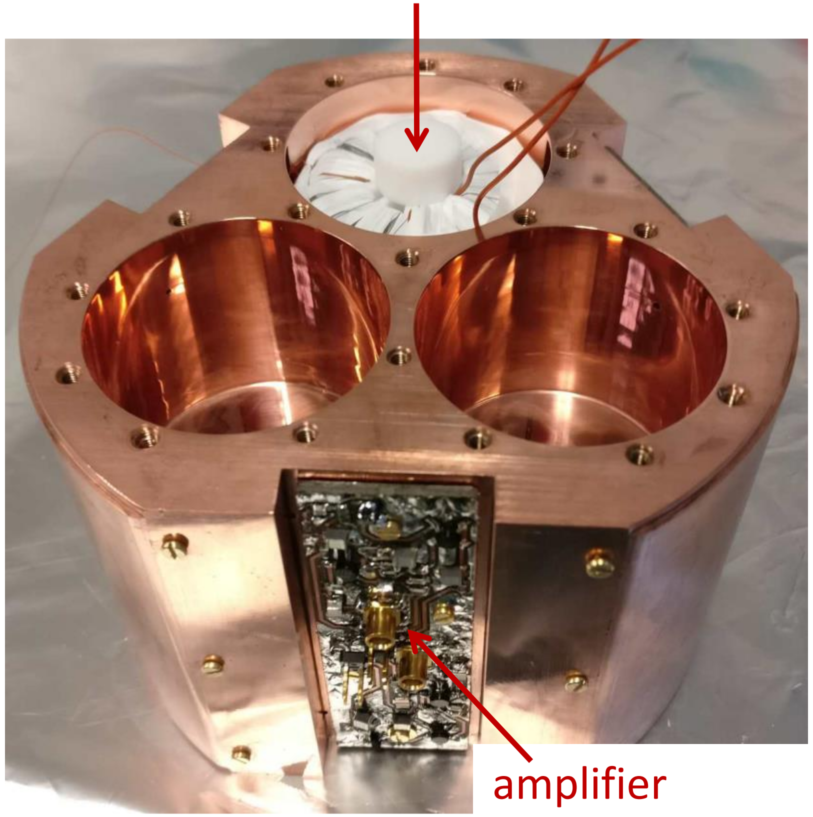

amplifier

Massive ^{165}Ho target

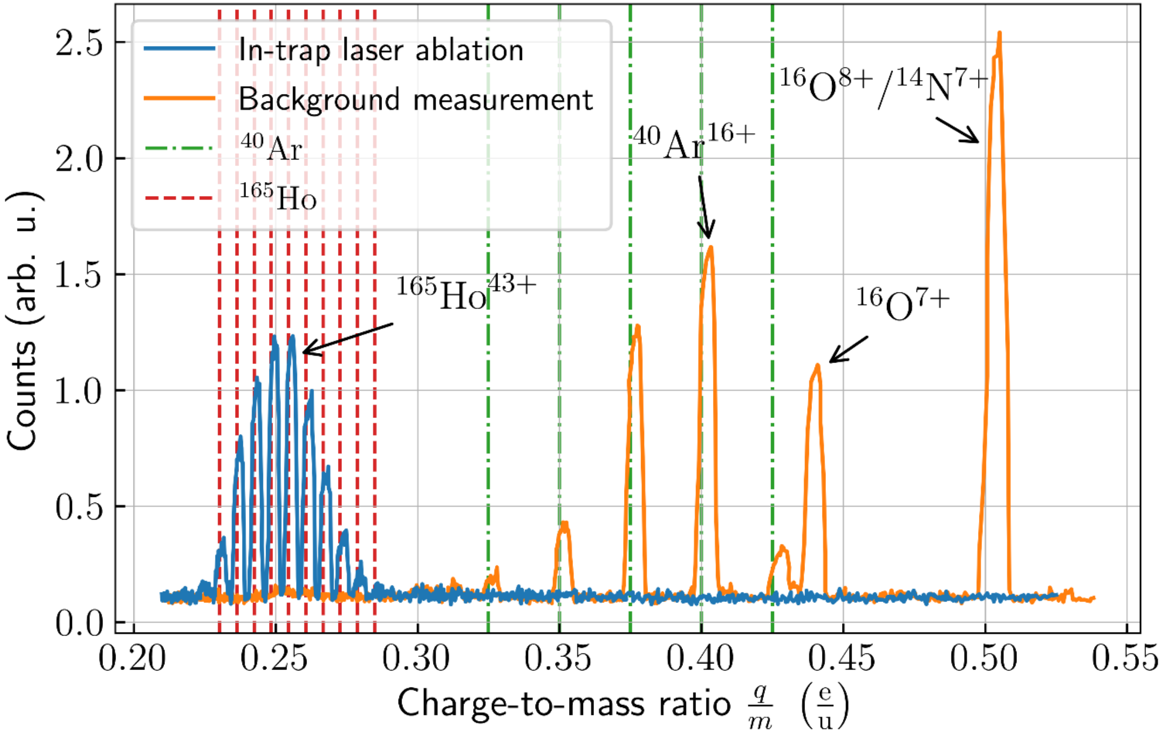

Blue curve: Laser ablation from ^{165}Ho target
Orange curve: Background measurement without laser

Small holmium targets

- 1 mm diameter Ti-wire
- Targets with known number of ^{165}Ho atoms on the surface:

  Drop-on-demand inkjet printing technique (group of Ch. Düllmann @ JGU Mainz)

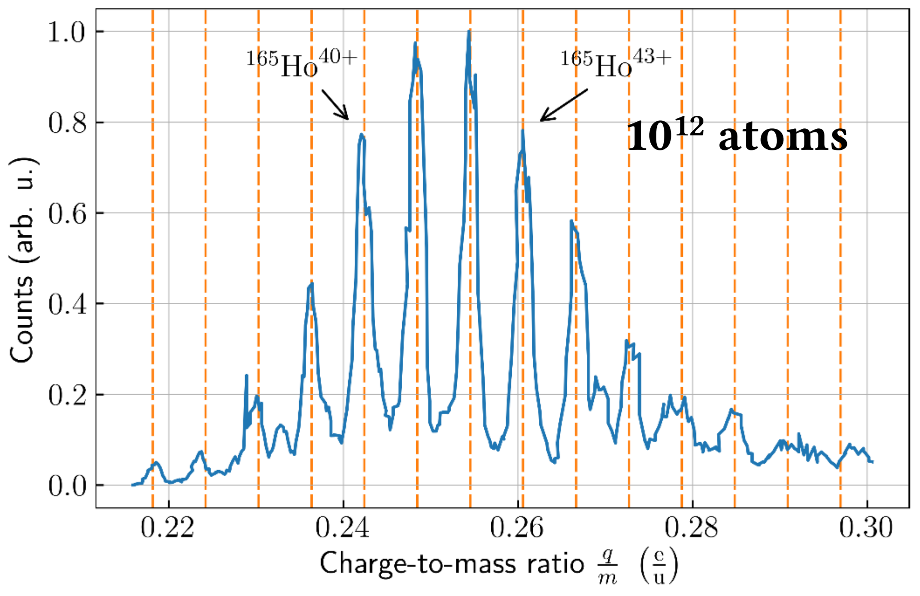

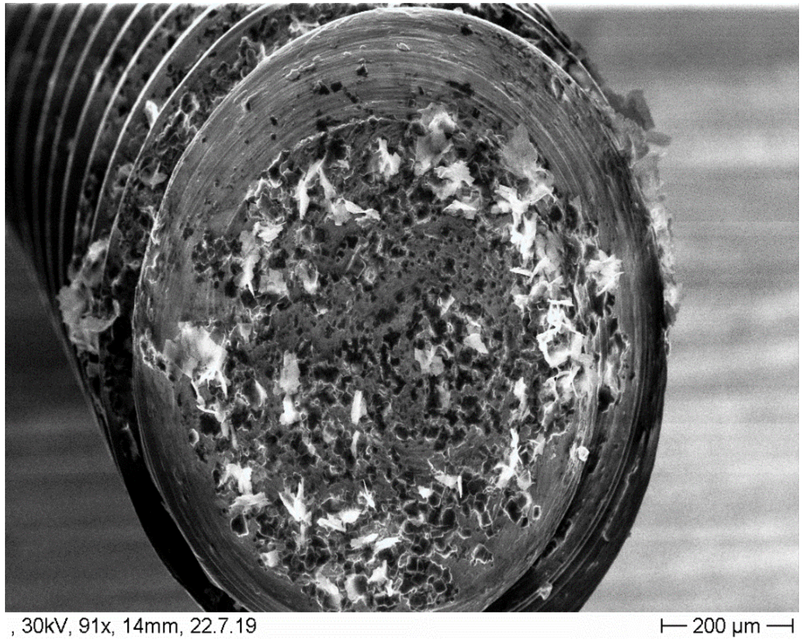

Targets for in-trap laser desorption

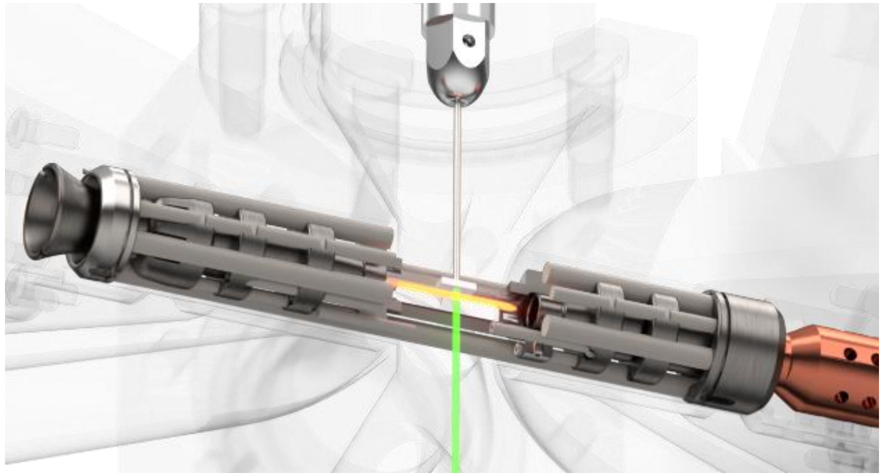

Target types:

- „Drop-on-demand“ printed targets: µg to ng samples, smallest target: 10^{12} atoms ^{165}Ho
- PLA-target: tens of µg to mg
- Massive targets: mg samples, e.g. metallic foil, bulk material

PLA, 30 µg Yb_2O_3

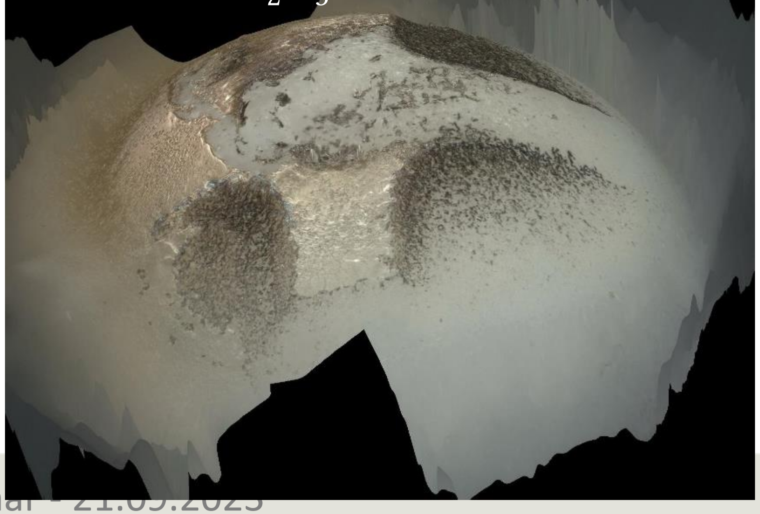

PLA with Yb_2O_3; > 200 k laser shots

Bradbury-Nielsen Gate: design

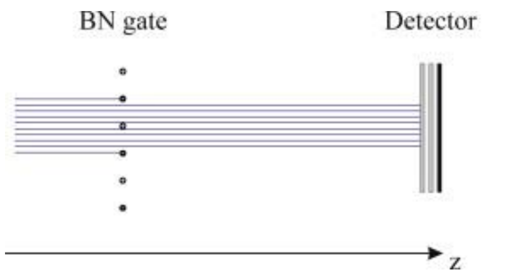

NO voltage applied

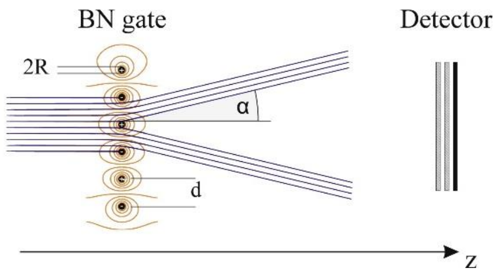

POS/NEG voltage applied

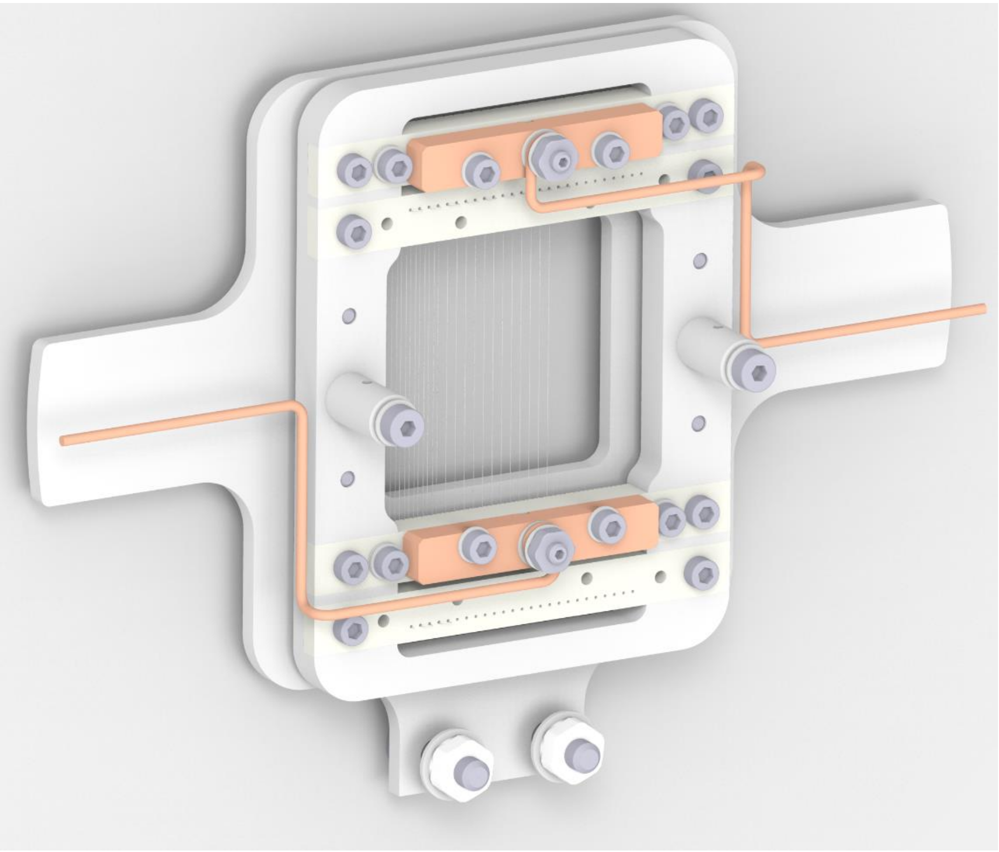

Wolf, R.N. et al., *NIMA 686, 82* (2012)
Brunner, T. et al., *IJMS 309*, 97 (2012)

Bradbury-Nielsen Gate: performance

1st version: 40 ns pulse width/20-30 ns jitter

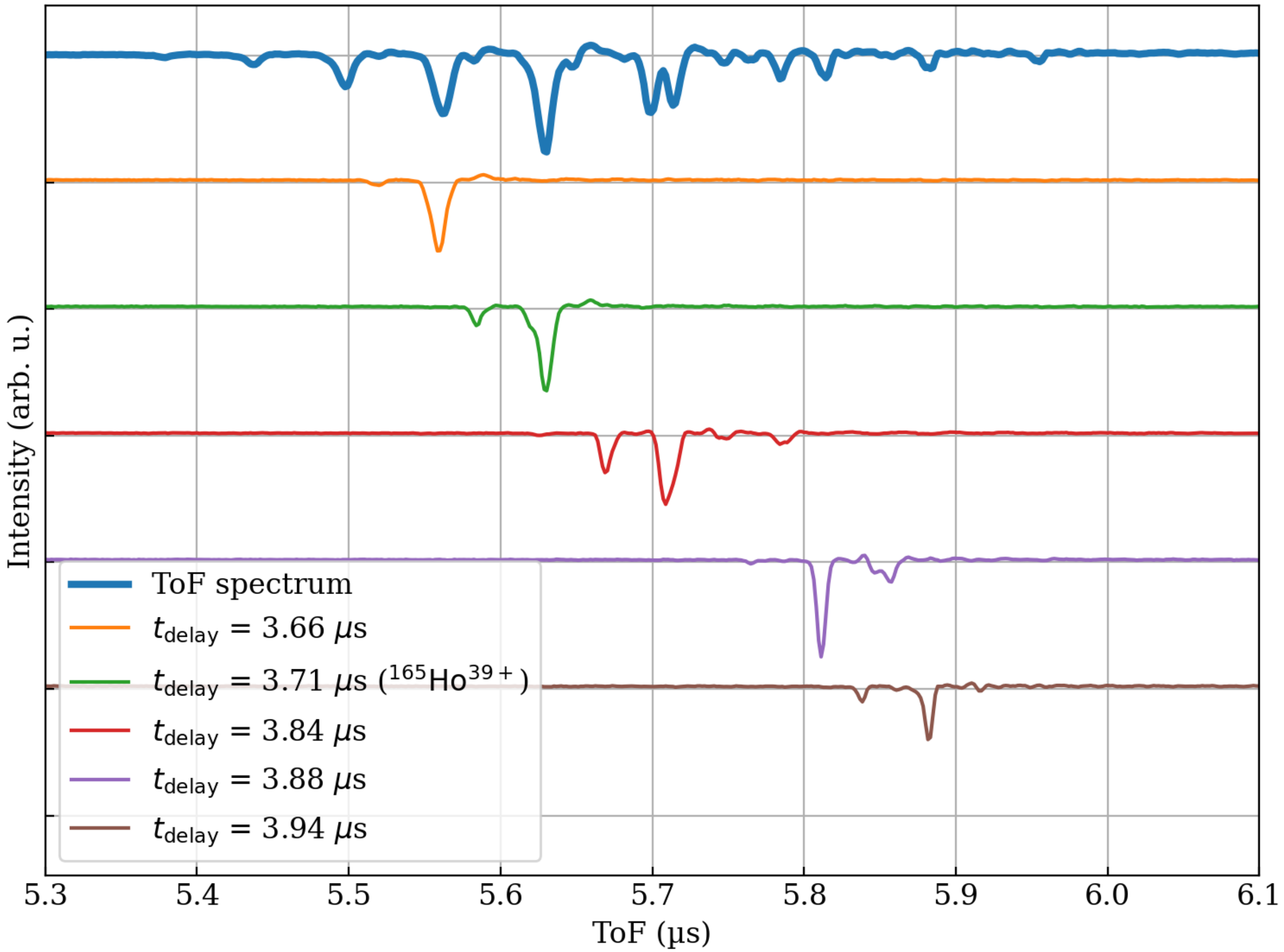

MOSFET switch for Bradbury-Nielsen Gate

- Switch based on two N-channel MOSFETs with gate drivers
- Pulse width reduced from 40 to 20 ns
- Near future: Faster MOSFETs placed inside the vacuum chamber

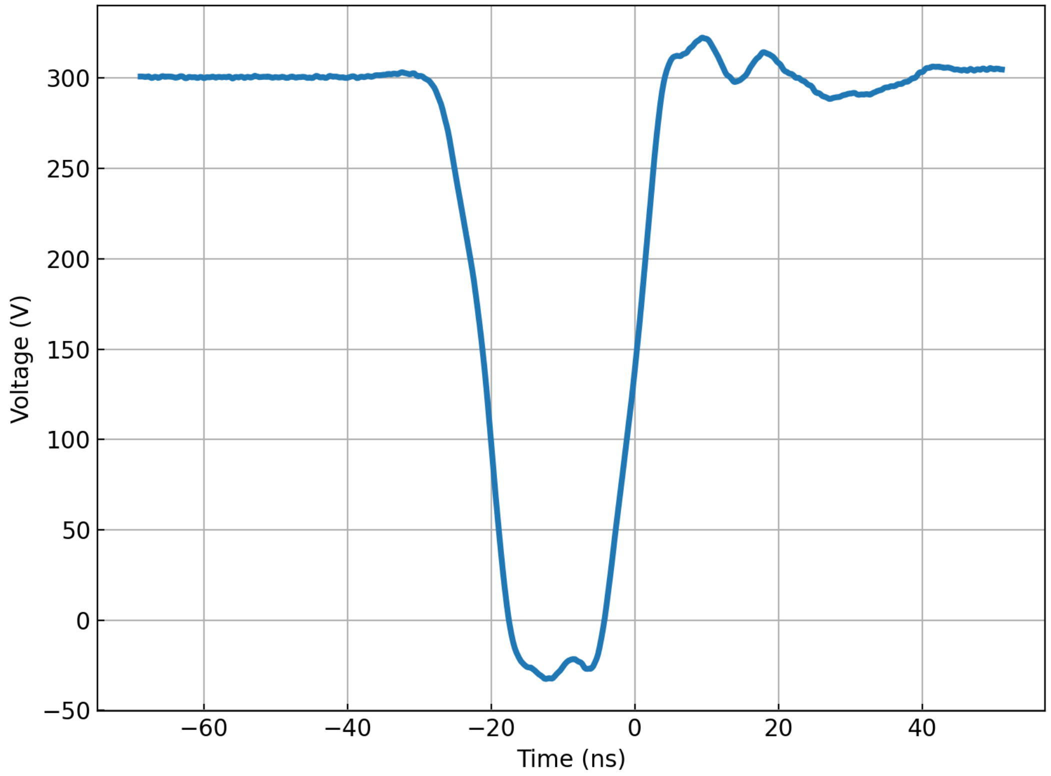

newest design ~20 ns pulse width

Measurement of trap frequencies with PENTATRAP

$$I_{ion}^{max} = 2\pi\nu_z q \frac{z_{max}}{D} = 15\ fA$$

$$z_{max} = 10\ \mu m$$

$$\nu_z = 500\ kHz$$

$$Re^{29+}$$

$$R_{LC} = 2\pi\nu_{LC} LQ = 25\ MOhm$$

$$L = 1.5\ mH$$

$$Q = 5000$$

$$U_{ion}^{max} = I_{ion}^{max} R_{LC} = 370\ nV$$

$$U_{th\_4K} = 70\ \mathrm{nV}$$

$$U_{th\_300K} = 600\ \mathrm{nV}$$

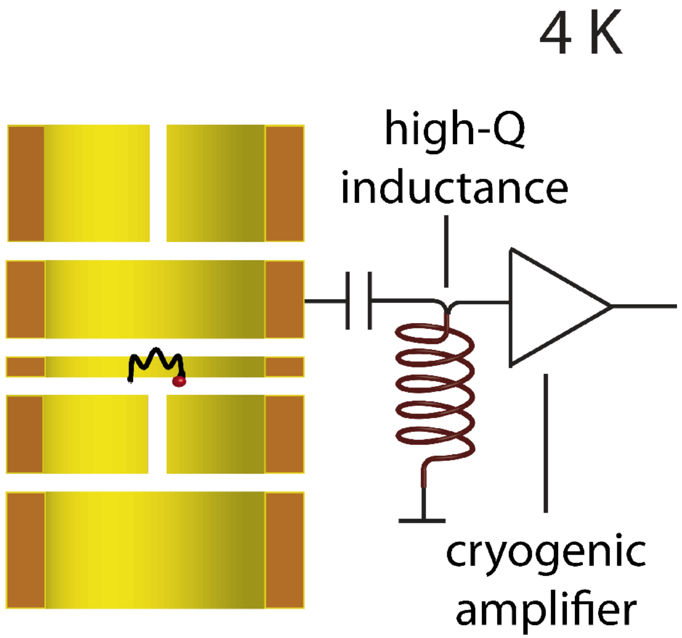

Determination of Q-value of β^- -decay of ^{187}Re

$$Q = M[^{187}\mathrm{Re}] - M[^{187}\mathrm{Os}] = M[^{187}\mathrm{Os}^{29+}]\cdot[R-1]+\Delta B$$

Maurits Haverkort
Heidelberg University Institute for Theoretical Physics
Zoltan Harman
Max-Planck Institute for Nuclear Physics
Paul Indelicato
Directeur de Recherche au CNRS

A multiconfiguration Dirac-Hartree-Fock method (MCDHF) ,
a fully relativistic approach, and its combination with Brillouin-Wigner many-body perturbation theory are used.

The ground state of the Re^{29+}ion is a simple Pd-like configuration [Kr]$4d^{10}$ $^1S_0$,
the neutral Re atom is in the [Xe]$4f^{14}5d^5 6s^2$ $^6S_{5/2}$ electronic state.

The Os ion and atom have an additional electron compared to their Re counterparts, thus their ground states are the Ag-like [Kr]$4d^{10}4f$ $^2F_{5/2}$ and [Xe]$4f^{14}5d^6 6s^2$ $^5D_4$ configurations, respectively.

Within the MCDHF scheme, the many-electron atomic state function is given as a linear combination of configuration state functions (CSFs) with a common total angular momentum (J), magnetic (M) and parity (P) quantum numbers: $|\Gamma PJM\rangle = \sum_k c_k |\gamma_k PJM\rangle$. The CSFs $|\gamma_k PJM\rangle$ are constructed as jj-coupled Slater determinants of one-electron orbitals, and γ_k summarizes all the information needed to fully define the CSF, i.e. the orbital occupation and coupling of single-electron angular momenta. Γ collectively denotes all the γ_k included in the representation of the ground state.

The GRASP2018 code package [30] is used.

^{163}Ho wire preparation

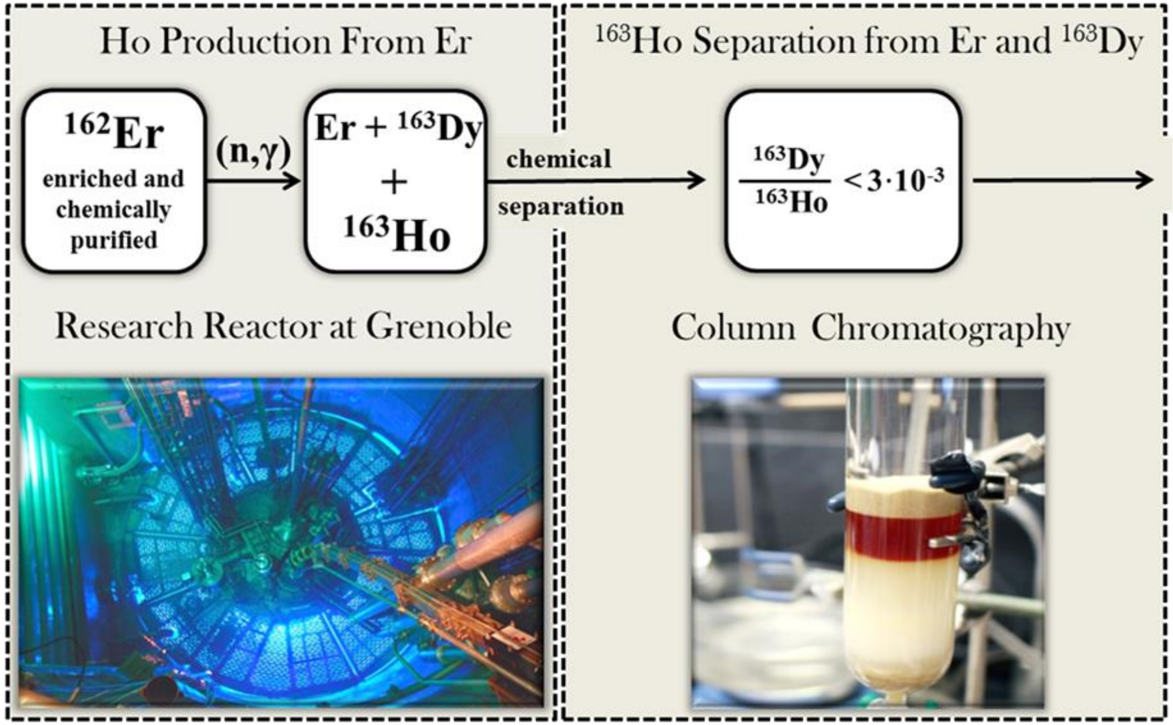

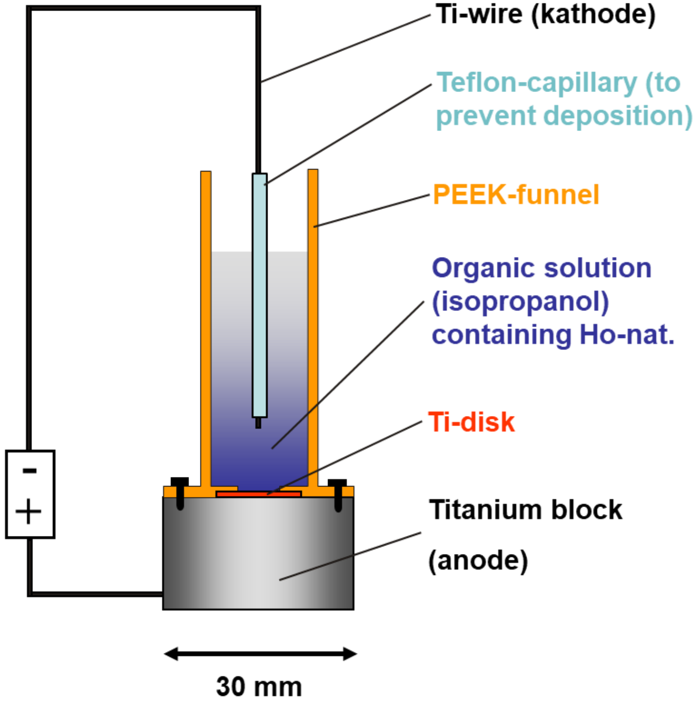

atomic metastable states in Re^{29+} and Os^{30+}

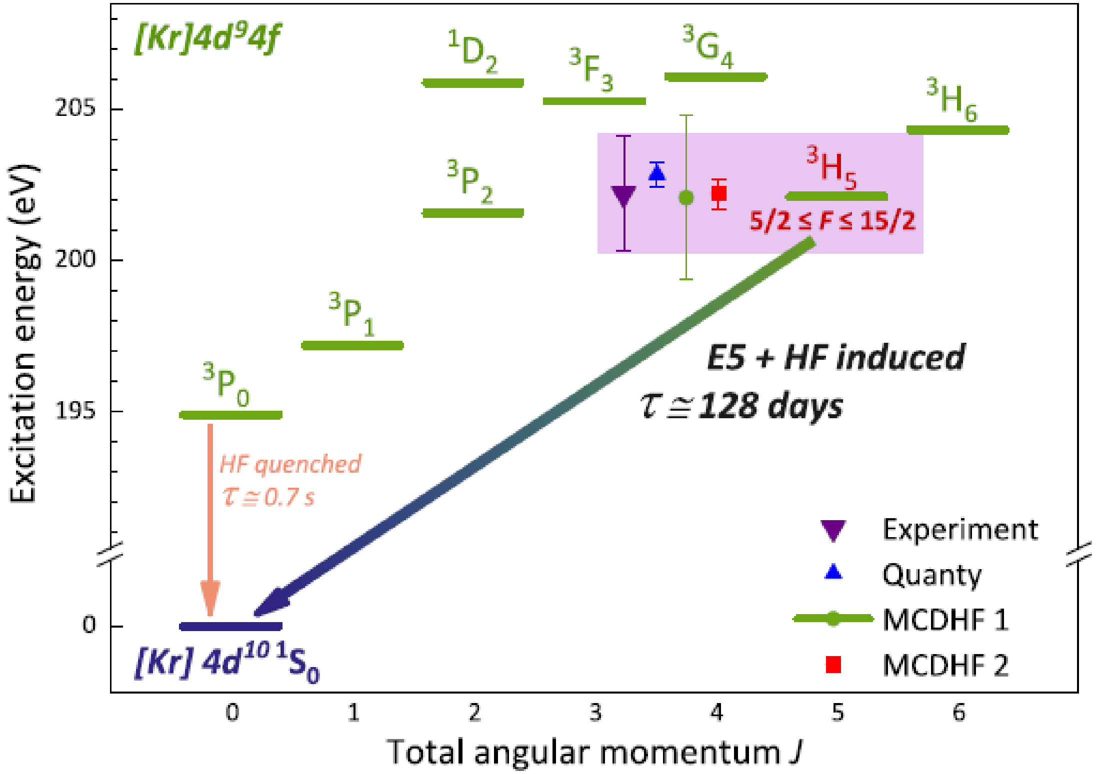

Figure 2: The $4d^{10}$ ground state and relevant $4d^94f$ excited electronic states of the $^{187}Re^{29+}$ ion. Comparison of the experimental result and theoretical values obtained using multi-configuration Dirac-Hartree Fock approaches in two different implementations (MCDHF 1 and 2) and by means of a configuration-interaction (Quanty) calculation is shown in the coloured bar.

^{168,170,172,174,176}Yb

I. Counts et al., PRL 125, 123002 (2020) (MIT, USA)

Measurement: two quadrupole transitions in 5 Yb$^+$ Isotopes, $6s^2S_{1/2} \leftrightarrow 5d^2D_{5/2}$ (411 nm), $6s^2S_{1/2} \leftrightarrow 5d^2D_{3/2}$ (436 nm) with an uncertainty of 300 Hz (limited by laser drift).

Method: ion in Paul trap; Doppler cooled on $6s^2S_{1/2} \rightarrow 6p^2P_{1/2}$ to 0.5 mK; coherent Ramsey spect./electron-shelving scheme.

Results: King plot shows a $3 \cdot 10^{-7}$ deviation from linearity at 3σ uncertainty level.

Indication of the fifth force or higher order nuclear effects within the SM.

Outlook: (statement in the paper)

In the future, the measurement precision can be increased by several orders of magnitude by cotrapping two isotopes. This improvement, also in combination with measurements on additional transitions, such as the $^2S_{1/2} \rightarrow {}^2F_{7/2}$ octupole transition in Yb$^+$ or
clock transitions in neutral Yb, will allow one to discriminate between nonlinearities of different origin.

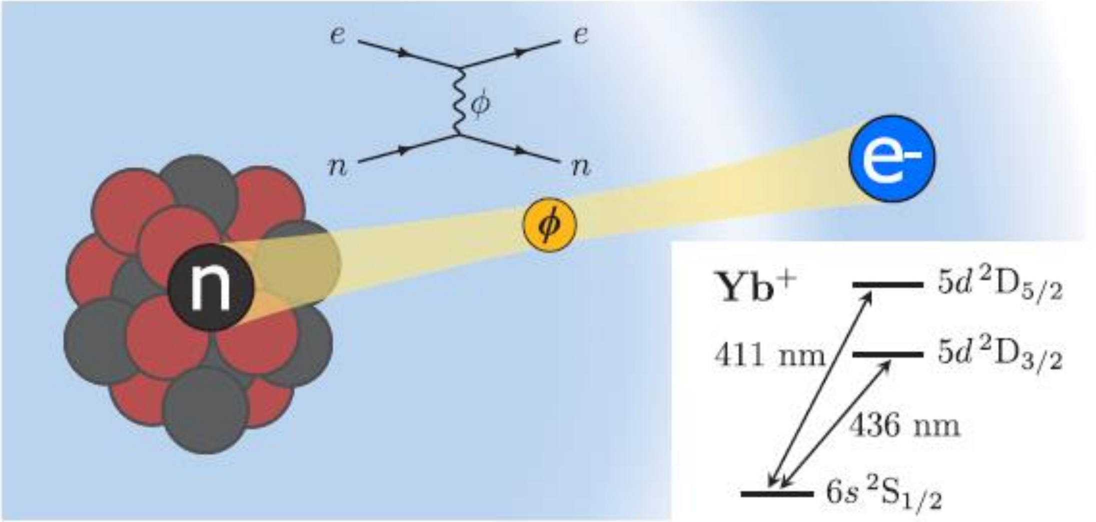

taken from the paper

$^{168,170,172,174,176}Yb$

I. Counts et al., PRL 125, 123002 (2020) (MIT, USA)

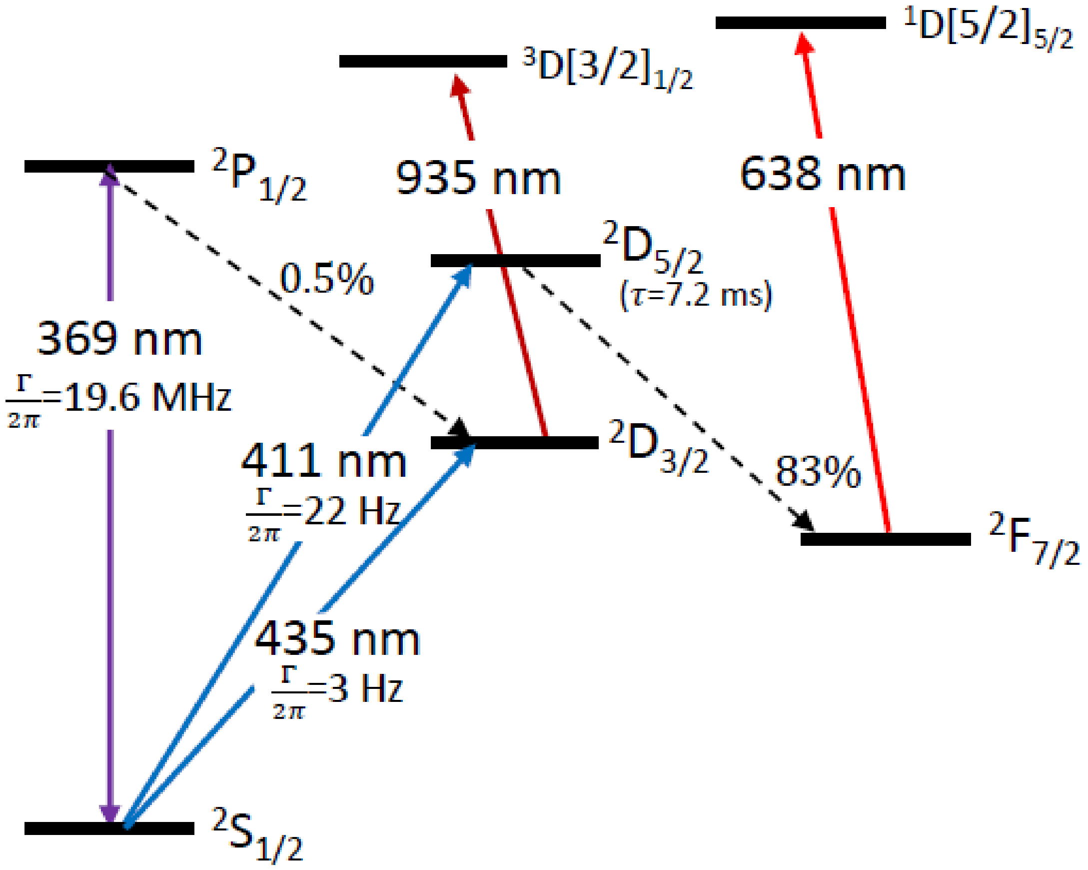

FIG. S1. Partial Yb$^+$ level diagram.

taken from the paper

dark matter and 5th force

$^{40,42,44,46,48}Ca$

C. Solaro et al., PRL 125, 123003 (2020) (Aarhus University, Denmark)

F.W. Knollmann et al., PRA 100, 022514 (2019) (Williams College, USA)

Measurement: two quadrupole transitions in 5 Ca^+ Isotopes, $4s^2S_{1/2} \leftrightarrow 3d^2D_{5/2}$ (729 nm) , $4s^2S_{1/2} \leftrightarrow 3d^2D_{3/2}$ (732 nm) with an uncertainty of 20 Hz.

Method: (1) frequency-comb Raman spectroscopy on $3d^2D_{3/2} \leftrightarrow 3d^2D_{5/2}$ (C. Solaro et al.)
(2) co-trapped ions in a Paul trap, laser spectroscopy on $4s^2S_{1/2} \leftrightarrow 3d^2D_{5/2}$ (729 nm) (F.W. Knollmann et al.)

Results: no non-linearity of the King's plot is observed.

Outlook:

D-D transitions with 10 mHz accuracy, S-D with 1 Hz.

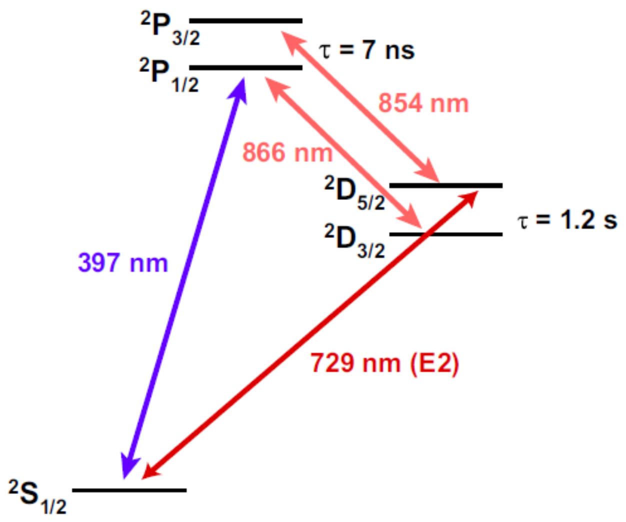

FIG. 1. Level diagram for nuclear spin-zero isotopes of Ca^+, with natural lifetimes listed. The 397-nm transition is used for Doppler cooling and fluorescence detection, while metastable $^2D_{3/2,5/2}$ levels are repumped by transitions at 866 and 854 nm, respectively.

taken from the paper by F.W. Knollmann

Raman spectroscopy

A Raman transition couples two atomic levels by the absorption of a photon from one Raman beam (pump beam) and by stimulated emission of another one into the other beam (Stokes beam).

The narrow linewidth of Raman transitions can be used to resolve atomic motional sidebands.

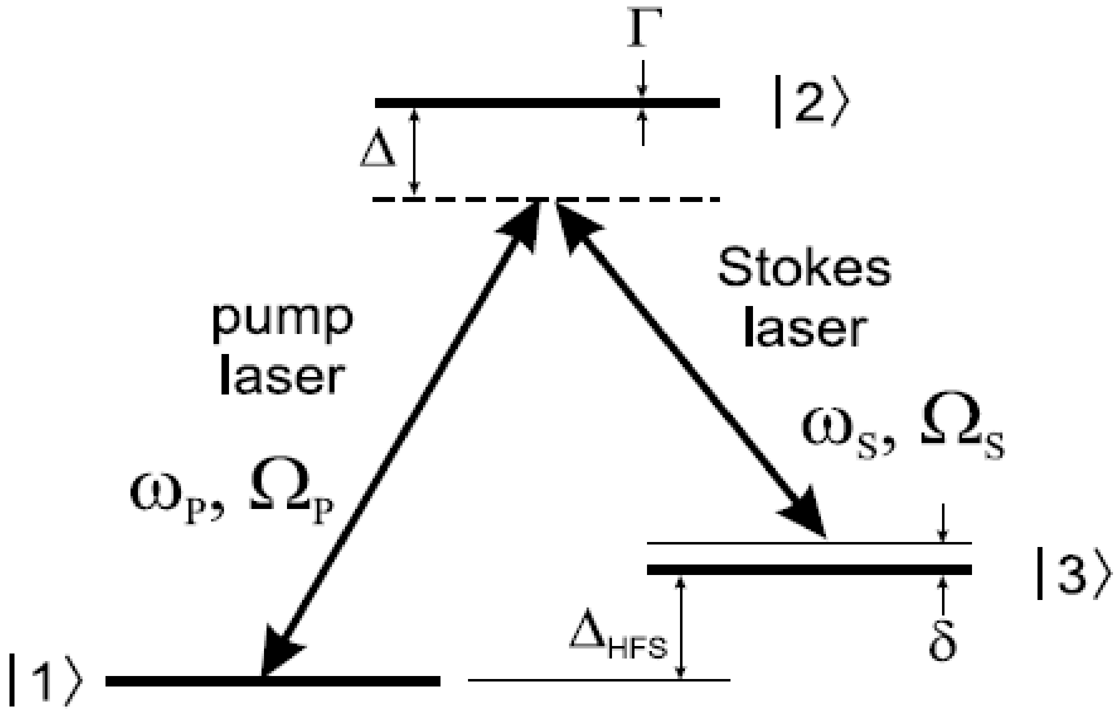

$^{84,86,87,88,90}Sr$

T. Manowitz et al., PRL 123, 203001 (2019) (Weizmann Institute of Science, Israel)

H. Miyake et al., PRR 1, 033113 (2019) (Joint Quantum Institute, USA)

Measurement: (1) $^1S_0$– $^3P_1$ (689 nm, linewidth=7.4 kHz), $^1S_0$– $^3P_0$ (698 nm, linewidth= mHz), with an uncertainty of a few kHz.

(2) electric quadrupole (0.4 Hz) $^5S_{1/2}$ – $^4D_{5/2}$ with an uncertainty of 9 mHz.

Method: (1) laser spectroscopy in optical dipole trap.

(2) decoherence free subspaces (DFSs). Direct probe of the isotope shift with 9 mHz uncertainty.

Results: nonlinearity in the measured values. The problem may be ^{87}Sr (center of hyperfine splitting is determined wrongly).

^{90}Sr is needed (radioactive, 29 years life time).

Outlook:

Method of decoherence free subspaces with all isotopes.

dark matter and 5th force

$^{130,132,134,136,138}Ba$

P. Imgram et al., PRA 99, 012511 (2019) (TU Darmstadt, Germany)

Measurement: $6s^2S_{1/2} - 6p^2P_{1/2}$ (D1, 493 nm), $6s^2S_{1/2} - 6p^2P_{3/2}$ (D2, 455 nm), with accuracy of 200 kHz.

Method: collinear/anticollinear laser spectroscopy on collimated fast ion beams.

Results: uncertainty comparable to ion trap measurements on dipole transitions but far from the needed one for 5th force.

$^{142,144,146,148,150}Nd$

N. Bhatt et al., ArXiv 2002.08290 (Uni of Toronto, Canada)

Measurement: $4f^46s$ - $[25044.7]_{7/2}$ (399 nm), $4f^46s$ - $[25138.6]_{7/2}$ (397 nm) with accuracy of a few 100 kHz.
Method: laser absorption spectroscopy of cold ions in a neutral plasma.

Results: uncertainty comparable to ion trap measurements on dipole transitions but far from the needed one for 5th force.

Outlook:

several telecommunication forbidden transitions 1500 nm with sub-Hz uncertainty.

Stabilization of LHe level and He pressure

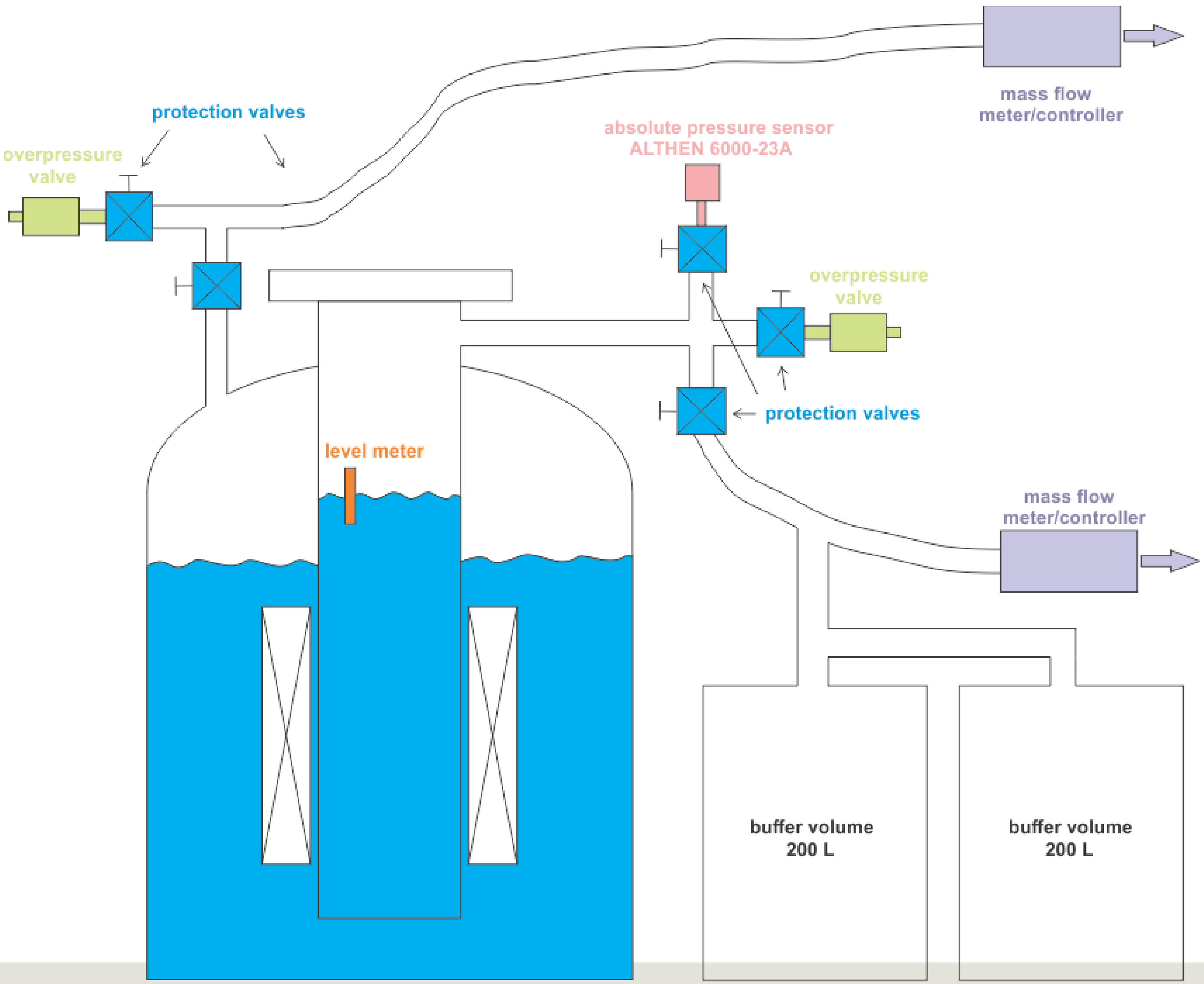

Polynomial Method

Ann. Inst. Statist. Math.
30 (1978), Part A, 9-14

A BAYESIAN ANALYSIS OF THE MINIMUM AIC PROCEDURE

HIROTUGU AKAIKE

(Received Oct. 15, 1977; revised Apr. 24, 1978)

Summary

By using a simple example a minimax type optimality of the minimum AIC procedure for the selection of models is demonstrated.

Biometrika (1989), **76**, 2, *pp.* 297-307
Printed in Great Britain

Regression and time series model selection in small samples

BY CLIFFORD M. HURVICH
Department of Statistics and Operations Research, New York University, New York NY 10003, U.S.A.

AND CHIH-LING TSAI
Division of Statistics, University of California, Davis, California 95616, U.S.A.

SUMMARY

A bias correction to the Akaike information criterion, AIC, is derived for regression and autoregressive time series models. The correction is of particular use when the sample size is small, or when the number of fitted parameters is a moderate to large fraction of the sample size. The corrected method, called $\mathrm{AIC_C}$, is asymptotically efficient if the true model is infinite dimensional. Furthermore, when the true model is of finite dimension, $\mathrm{AIC_C}$ is found to provide better model order choices than any other asymptotically efficient method. Applications to nonstationary autoregressive and mixed autoregressive moving average time series models are also discussed.

dark matter and 5th force

$$\nu_i(\text{isotope}_1) - \nu_i(\text{isotope}_2) \equiv \Delta\nu_i = K_i \cdot \frac{m_1 - m_2}{m_1 m_2} + F_i \cdot [\langle r^2 \rangle_1 - \langle r^2 \rangle_2] + [\text{higher-order SM effects + LDM bosons}]$$

cannot be measured precisely

$$\Delta\nu_i = C_1 \cdot \frac{m_1 - m_2}{m_1 m_2} + C_2 \cdot \Delta\nu_j + [\text{higher-order SM effects + LDM bosons}]$$

King's plot

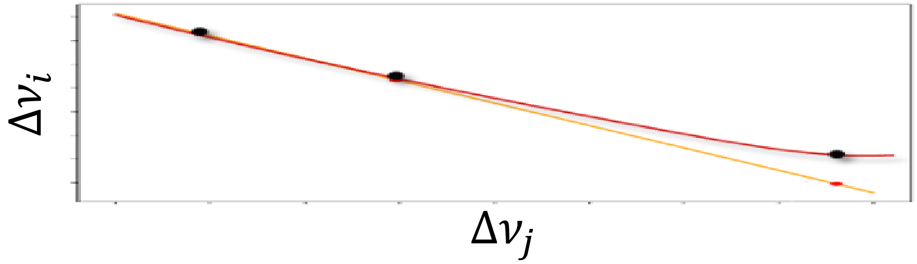

one needs elements with many even-even isotopes and quadrupole (narrow optical) transitions:

^{168,170,172,174,176}Yb	$^2S_{1/2} \leftrightarrow {}^2D_{5/2}$ (411 nm) $^2S_{1/2} \leftrightarrow {}^2D_{3/2}$ (436 nm)	I. Counts et al., PRL 125, 123002 (2020)
^{40,42,44,46,48}Ca	$4s^2S_{1/2} \leftrightarrow 3d^2D_{5/2}$ (729 nm) $4s^2S_{1/2} \leftrightarrow 3d^2D_{3/2}$ (732 nm)	C. Solaro et al., PRL 125, 123003 (2020) F.W. Knollmann et al., PRA 100, 022514 (2019)
^{84,86,88,90}Sr	$5S_{1/2} - 4D_{5/2}$ $1S_0 - 3P_1$, $1S_0 - 3P_0$	T. Manowitz et al., PRL 123, 203001 (2019) H. Miyake et al., PRR 1, 033113 (2019)

^{142,144,146,148,150}Nd	^{130,132,134,136,138}Ba
N. Bhatt et al., ArXiv 2002.08290	P. Imgram et al., PRA 99, 012511 (2019)

FUTURE:

$$\delta(\Delta\nu_i) \approx 10\ \text{mHz}$$

$$\delta\left(\frac{m_1}{m_2}\right) < 10^{-11}$$

The Electron Capture in Holmium experiment

$$\frac{dN}{dE} = A(Q - E)^2 \sqrt{1 - \frac{m_\nu^2}{(Q-E)^2}} \sum C\phi_k^2(0) \frac{\Gamma_k/2\pi}{(E - B_k)^2 + \Gamma_k^2/4}$$

$$Q_{\text{microcalorimetry}} \xrightarrow{\delta Q \sim \text{few eV}} \Delta Q \xleftarrow{\delta Q \sim \text{few eV}} Q_{\text{Penning trap}}$$

$$\Delta Q \downarrow \delta m_\nu^{\text{sys}}$$

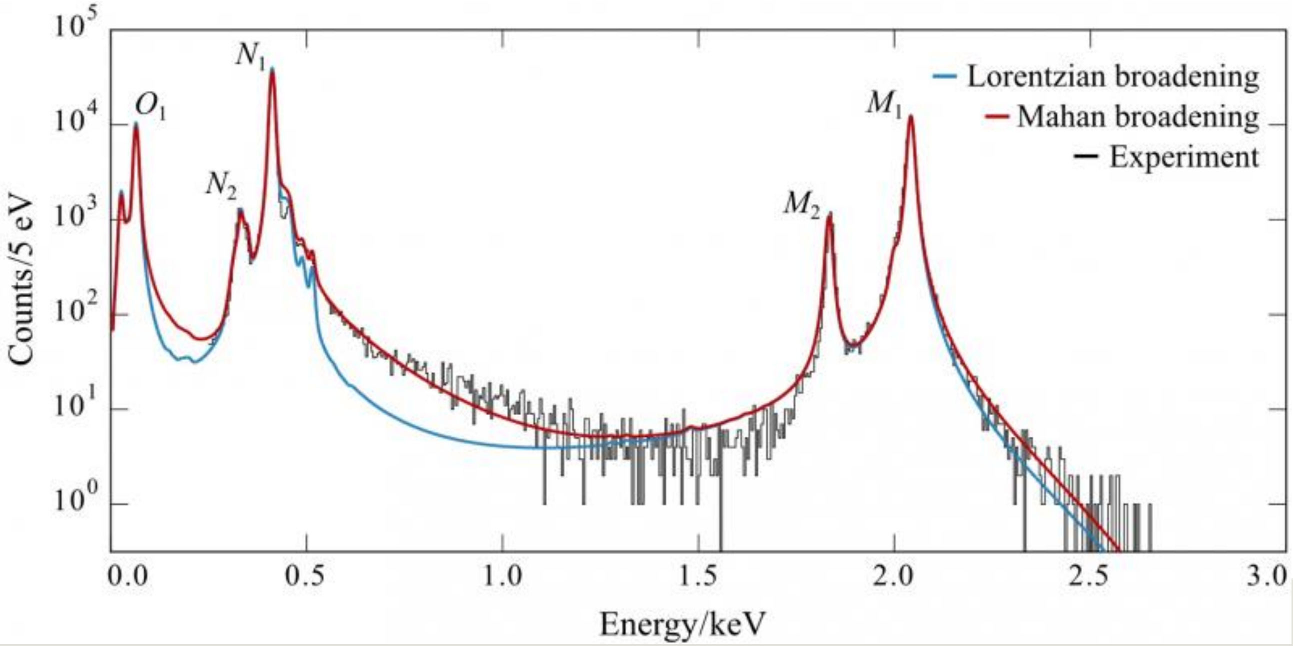

C. Velte et al. Eur. Phys. J. C (2019) 79: 1026

excitation energies of atomic metastable states

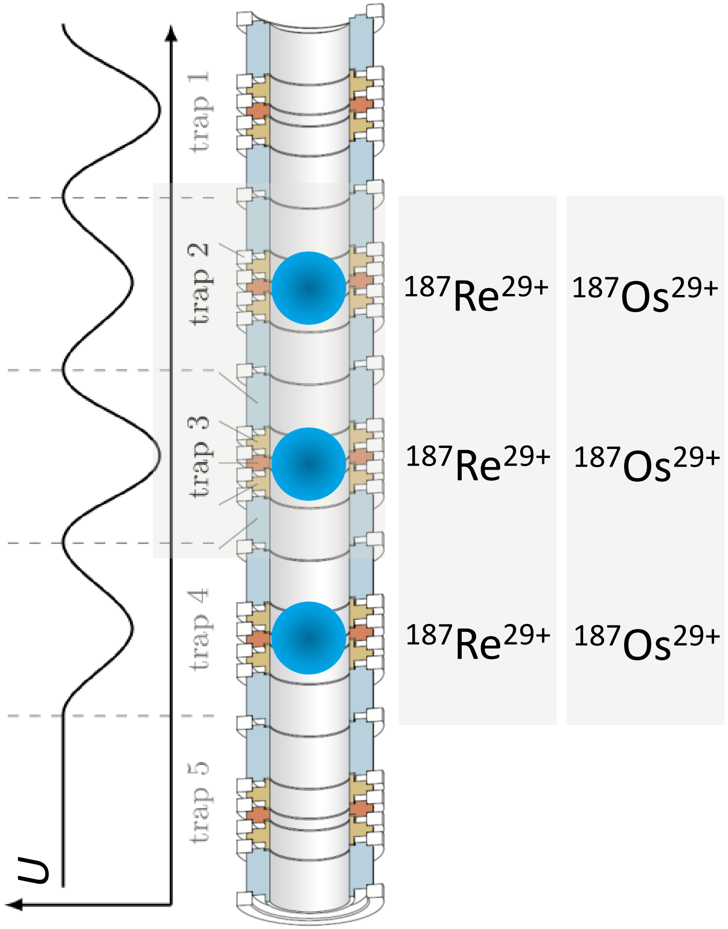

- Os^{29+} vs. Os^{29+} measurements yield always unity.
- Re^{29+} vs. Re^{29+} measurements yield either unity or $1+1.14\cdot10^{-9}$.

Re^{29+}

metastable state $[_{36}Kr]\ 4d^9\ 4f^1$

E5 (~128 days)

$B_{\text{PENTATRAP}}$ = 202.2(19) eV
B_{Harman} = 202.2(5) eV
$B_{\text{Indelicato}}$ = 202.1 (27) eV
$B_{\text{Haverkort}}$ = 202.8(4) eV

ground state $[_{36}Kr]\ 4d^{10}$

Os^{30+}

metastable state $[_{36}Kr]\ 4d^9\ 4f^1$

E5 (~128 days)

$B_{\text{PENTATRAP}}$ = 207(3) eV
$B_{\text{Haverkort}}$ = 209(2) eV
$B_{\text{Indelicato}}$ = 207(3) eV

ground state $[_{36}Kr]\ 4d^{10}$

Possible application: search for suitable clock transitions

R. Schüssler et al., *Nature* 581, 42 (2020)

Data Analysis: Polynomial Method